The *Vibrio cholerae* quorum-sensing protein VqmA integrates cell density, environmental, and host-derived cues into the control of virulence

Authors: Ameya A. Mashruwala[1,2], Bonnie L. Bassler[1,2#]

Affiliations:

[1]Department of Molecular Biology, Princeton University, Princeton, New Jersey 08544, USA.

[2]The Howard Hughes Medical Institute, Chevy Chase, MD 20815, USA.

[#]Correspondence to: bbassler@princeton.edu

Scientific Abstract

Quorum sensing is a chemical communication process in which bacteria use the production, release, and detection of signal molecules called autoinducers to orchestrate collective behaviors. The human pathogen *Vibrio cholerae* requires quorum sensing to infect the small intestine. There, *V. cholerae* encounters the absence of oxygen and the presence of bile salts. We show that these two stimuli differentially affect quorum-sensing function and, in turn, *V. cholerae* pathogenicity. First, during anaerobic growth, *V. cholerae* does not produce the CAI-1 autoinducer, while it continues to produce the DPO autoinducer, suggesting that CAI-1 may encode information specific to the aerobic lifestyle of *V. cholerae*. Second, the quorum-sensing receptor-transcription factor called VqmA, that detects the DPO autoinducer, also detects the lack of oxygen and the presence of bile salts. Detection occurs via oxygen-, bile salts-, and redox-responsive disulfide bonds that alter VqmA DNA binding activity. We propose that VqmA serves as an information processing hub that integrates quorum-sensing information, redox status, the presence or absence of oxygen, and host cues. In response to the information acquired through this mechanism, *V. cholerae* appropriately modulates its virulence output.

Importance/Lay Abstract

Quorum sensing (QS) is a process of chemical communication bacteria use to orchestrate collective behaviors. QS communication relies on chemical signal molecules called autoinducers. QS regulates virulence in *Vibrio cholerae*, the causative agent of the disease cholera. Transit into the human small intestine, the site of cholera infection, exposes *V. cholerae* to the host environment. In this study, we show that the combination of two stimuli encountered in the small intestine, the absence of oxygen and the presence of host-produced bile salts, impinge on *V. cholerae* QS function and, in turn, pathogenicity. We suggest that possessing a QS system that is responsive to multiple environmental, host, and cell density cues enables *V. cholerae* to fine-tune its virulence capacity in the human intestine.

Introduction:

Quorum sensing (QS) is a process of cell-cell communication that bacteria use to synchronize group behaviors such as bioluminescence, DNA exchange, virulence factor production, and biofilm formation (20, 39, 45, 56). QS depends on the production, release, accumulation, and group-wide detection of extracellular signaling molecules called autoinducers (AI) (45, 53). At low cell density (LCD), when there are few cells present and the concentration of AIs is low, the expression of genes driving individual behaviors occurs (45, 53, 59). As the cells grow to high cell density (HCD), the extracellular concentration of AIs likewise increases. Detection of accumulated AIs drives the population-wide expression of genes required for group behaviors.

Vibrio cholerae is a Gram-negative enteric pathogen that causes infectious gastroenteritis. In *V. cholerae*, QS regulates collective behaviors including virulence factor production and biofilm formation (27, 39, 68, 69). Specifically, at LCD, genes encoding virulence factors and those required for biofilm formation are expressed (39). At HCD, genes required for both of these traits are repressed by QS (39). This pattern of gene expression is best understood in the context of the cholera disease. Infection is initiated by the ingestion of a small number of *V. cholerae* cells, and biofilm formation and virulence factor production are required for successful colonization (68, 69). In the host, the growth-dependent accumulation of AIs launches the HCD QS program, which

53 suppresses virulence factor production and biofilm formation, and triggers dispersal of
54 the bacteria back into the environment. Indeed, *V. cholerae* strains "locked" into the
55 LCD QS mode are more proficient in host colonization than strains "locked" in the HCD
56 QS mode (27). Thus, QS is proposed to be crucial for *V. cholerae* transitions between
57 environmental reservoirs and human hosts.

58 *V. cholerae* produces and detects three AIs, called AI-2, CAI-1 and DPO (Figure
59 1) (21, 39, 47, 54). CAI-1 is used for intra-genus communication while AI-2 and DPO
60 are employed for inter-species communication (5, 39, 47). Different combinations of the
61 three AIs are thought to allow *V. cholerae* to distinguish the number of vibrio cells
62 present relative to the total bacterial consortium. *V. cholerae* uses the information
63 encoded in blends of AIs to tailor its QS output depending on whether vibrios are in the
64 minority or the majority of a mixed-species population (5, 39).

65 AI-2 and CAI-1 are detected by membrane-bound receptors LuxPQ and CqsS,
66 respectively. The receptors funnel information into a shared regulatory pathway (Figure
67 1) (21, 39). DPO is detected by the cytoplasmic VqmA receptor-transcription factor that
68 activates expression of *vqmR*, encoding the VqmR regulatory small RNA (sRNA) (34,
69 46, 47). Both Apo- and DPO-bound-VqmA (Holo-VqmA) can activate *vqmR* expression
70 with Holo-VqmA being more potent than Apo-VqmA (22). VqmR post-transcriptionally
71 regulates target mRNAs (46). Important to this study is that at HCD, all three QS
72 systems repress genes required for virulence and biofilm formation (Figure 1).

73 Upon the transition from the marine niche to the human host, *V. cholerae*
74 switches from an aerobic to an anaerobic environment (15, 66). In addition, it
75 encounters bile, which is abundant in the lower intestine, the primary site of *V. cholerae*
76 infection. Bile is a heterogeneous mixture of compounds, including electrolytes and bile
77 acids, and is estimated to be present at ~0.2-2% weight/volume of intestinal contents
78 (14). Bile salts are known to affect *V. cholerae* virulence gene expression by modulating
79 activities of the oxidoreductase DsbA, the transmembrane-spanning transcription factor
80 TcpP, and the ToxT transcription factor (6, 9, 23, 60, 64, 65). Bile salts also promotes
81 biofilm formation in *V. cholerae*, and the second messenger molecule called cyclic-di-
82 guanylate is involved in mediating this effect (24, 29).

83 Here, first we explore whether oxygen levels modulate QS in *V. cholerae*. We
84 find that *V. cholerae* cultured under anaerobic conditions does not produce CAI-1,
85 whereas increased DPO production does occur. In this work we focus on DPO. We
86 show that the VqmA-DPO complex more strongly activates target gene expression
87 under anaerobic than aerobic conditions. One consequence of the absence/presence of
88 oxygen is an altered reducing/oxidizing (hereafter, redox) cellular environment. We
89 show that oxygen-dependent changes in VqmA activity are governed by cysteine
90 disulfide bonds that are responsive to the redox environment. In the absence of DPO,
91 during aerobic growth, Apo-VqmA forms an intra-molecular disulfide-bond that limits
92 VqmA activity. By contrast, DPO-bound VqmA forms an inter-molecular disulfide-bond
93 that enhances VqmA activity, and indeed, this inter-molecular disulfide bond was also
94 shown to be present in a recently reported crystal structure of Holo-VqmA (63). The
95 formation of the inter-molecular bond is not affected by oxygen levels. In the small
96 intestine, *V. cholerae* encounters both the absence of oxygen and the presence of bile.
97 Bile salts inhibit formation of the inter-molecular disulfide bond in VqmA. Thus, bile and
98 DPO have opposing effects on VqmA-DPO activity. We propose that the VqmA-DPO-
99 VqmR QS pathway allows *V. cholerae* to integrate QS information, host cues, and
100 environmental stimuli into the control of genes required for transitions between the
101 human host and the environment.
102
103 **Results:**
104 ***V. cholerae* does not produce the CAI-1 QS AI under anaerobic conditions**. To our
105 knowledge, *V. cholerae* QS has only been studied under aerobic conditions. We know
106 that the marine-human host lifecycle demands that *V. cholerae* transition between
107 environments containing widely varying oxygen levels (15, 66). Moreover, QS is crucial
108 in both *V. cholerae* habitats. Thus, we sought to investigate whether oxygen modulates
109 *V. cholerae* QS. First, we assessed the relative levels of the three known QS AIs from
110 *V. cholerae* C6706 Sm^R (hereafter wild-type; WT) following aerobic and anaerobic
111 growth. AI activity in cell-free culture fluids was measured using a set of three
112 bioluminescent *V. cholerae* strains, each of which exclusively reports on one QS AI
113 (either AI-2, CAI-1, or DPO) when it is supplied exogenously.

114 Unlike *V. cholerae* cultured in the presence of oxygen (hereafter +O_2), *V.*
115 *cholerae* grown in the absence of oxygen (hereafter -O_2) produced no CAI-1. Twice as
116 much AI-2 and DPO accumulated in *V. cholerae* cultured -O_2 than +O_2 (Figure 2A-C).
117 We note that the dynamic ranges for the CAI-1 and DPO assay are ~1,000- and ~4-fold,
118 respectively, while that for the AI-2 assay is ~100,000-fold (39, 47). Thus, we consider
119 the changes in CAI-1 and DPO to be physiologically relevant, whereas that for AI-2 is
120 likely not, so we do not consider AI-2 further in this work. Additionally, *V. cholerae*
121 cultured -O_2 grew to a lower final cell density than when grown +O_2 (Supplementary
122 Figure 1A). We controlled for the reduced cell growth that occurs in the -O_2 conditions,
123 nonetheless, no CAI-1 could be detected (Supplementary Figure 1B). Beyond lacking
124 O_2, our culture medium lacked an alternative terminal electron acceptor. Thus, we also
125 considered the possibility that *V. cholerae* cultured in -O_2 conditions was unable to
126 respire and therefore unable to drive CAI-1 generation. However, supplementation of
127 the *V. cholerae* -O_2 cultures with the alternative terminal electron acceptor fumarate,
128 which is readily consumed by *V. cholerae* (4), did not rescue CAI-1 production
129 (Supplementary Figure 1B). Collectively, these data suggest that production of CAI-1
130 and DPO by *V. cholerae* is affected by oxygen levels. In the remainder of this study, we
131 focus on the functioning of the DPO-VqmA QS circuit under different conditions that are
132 predicted to be encountered in the host. We address possible ramifications of our
133 results concerning CAI-1 and AI-2 in the Discussion.
134
135 **VqmA exhibits increased activity in the absence of oxygen.** Given that *V. cholerae*
136 accumulated more DPO under -O_2 conditions than +O_2 conditions, we wondered
137 whether the VqmA-DPO QS system would, in turn, display increased activity under -O_2
138 conditions compared to +O_2 conditions. VqmA controls the expression of the *vqmR*
139 gene, encoding the small RNA VqmR (Figure 1). Therefore, expression of a *vqmR-lacZ*
140 transcriptional fusion can be used to assess VqmA activity (47). Beta-galactosidase was
141 selected as the reporter because its activity is not affected by oxygen. The *vqmR-lacZ*
142 construct was integrated onto the chromosome of Δ*tdh V. cholerae*. Tdh (threonine
143 dehydrogenase) is required for DPO production (47). Thus, the

144 Δ*tdh* strain makes no DPO but activates *vqmR-lacZ* expression in response to
145 exogenously supplied DPO. We measured activity following growth in +O_2 and -O_2
146 conditions and in the absence and presence of exogenous DPO. In the presence of O_2,
147 *vqmR-lacZ* activity increased following supplementation with DPO (Supplementary
148 Figure 2A). Compared to the +O_2 conditions, *vqmR-lacZ* activity was higher under -O_2
149 conditions, both in the absence and presence of DPO (Supplementary Figure 2A).
150 Increased DPO-independent *vqmR-lacZ* expression in the absence of O_2 could be a
151 consequence of increased production of VqmA or increased VqmA activity. To
152 distinguish between these possibilities, we first examined whether changes in O_2 levels
153 alter VqmA production by quantifying VqmA-FLAG produced from the chromosome -
154 /+O_2 and -/+ DPO. Similar levels of VqmA-FLAG were produced in all cases, suggesting
155 that a change in VqmA abundance does not underlie increased *vqmR-lacZ* expression
156 under -O_2 conditions. (Supplementary Figure 2B). We next tested O_2-driven changes in
157 VqmA activity. To do this, we uncoupled expression of *vqmA-FLAG* from its native
158 promoter by cloning *vqmA-FLAG* onto a plasmid under an arabinose inducible promoter
159 (hereafter, p*vqmA-FLAG*). We introduced the plasmid into a Δ*vqmA* Δ*tdh V. cholerae*
160 strain harboring the *vqmR-lacZ* chromosomal reporter and we measured both β-
161 galactosidase output as well as VqmA-FLAG abundance in the same samples. VqmA-
162 FLAG levels did not change under the different conditions (Figure 3A), however, *vqmR-*
163 *lacZ* reporter activity normalized to cellular VqmA-FLAG levels increased in the cells
164 exposed to DPO, and overall activity was ~4-7-fold higher under -O_2 conditions than
165 +O_2 conditions both in the presence and absence of DPO (Figure 3B). We conclude that
166 VqmA displays an increased capacity to activate gene expression under anaerobic
167 conditions relative to aerobic conditions.
168
169 **VqmA forms intra- and inter-molecular disulfide bonds in an oxygen- and DPO-**
170 **dependent manner.** We wondered what molecular mechanism drives the increase in
171 VqmA activity under -O_2 conditions (Figure 3). The cytoplasmic compartment of
172 aerobically respiring *V. cholerae* is relatively oxidizing (35, 40). Thus, decreased oxygen
173 levels would shift the cytoplasm to a reducing environment (42). Proteins can respond
174 to such changes via redox-responsive cysteine residues (35, 38). Inspection of the

175 VqmA amino acid sequence revealed the presence of four cysteine residues and all are
176 strictly conserved in VqmA homologs in other vibrio species, but not in the VqmA
177 receptor recently discovered in a vibriophage (Supplementary Figure 3). These findings
178 led us to consider a model in which, in addition to activation by DPO, VqmA activity is
179 regulated by redox-responsive cysteine residues.

180 Cysteine residues often undergo disulfide bond formation (1, 38, 48). We
181 assessed whether VqmA forms disulfide bonds *in vivo* and, if so, whether their
182 formation is influenced by DPO and/or oxygen levels. We grew Δ*vqmA* Δ*tdh V. cholerae*
183 carrying the p*vqmA*-FLAG construct under +O_2 conditions. We subsequently divided the
184 culture into four aliquots. One portion was untreated (+O_2, -DPO), one portion was
185 supplied DPO (+O_2, +DPO), one portion was deprived of oxygen (-O_2, -DPO), and one
186 portion was deprived of oxygen and supplemented with DPO (-O_2, +DPO). We
187 extracted protein and analyzed the VqmA-FLAG protein profiles by immunoblot. These
188 analyses were performed with or without the addition of the reductant β-
189 mercaptoethanol (BME) to distinguish between VqmA-FLAG species that had and had
190 not formed disulfide bonds. Previous studies have shown that the presence of an intra-
191 molecular disulfide bond leads to a protein species displaying increased gel mobility
192 compared to the same protein lacking the bond (2, 55). By contrast, inter-molecular
193 disulfide bonds produce cross-linked protein oligomers that migrate with slower mobility
194 than the corresponding monomers (16, 44, 48). We first consider the results for VqmA
195 under +O_2 conditions: Under non-reducing conditions (-BME) and in the absence of
196 DPO, VqmA-FLAG displayed mobility consistent with an oxidized monomer (labeled O-
197 Monomer; Figure 4A and 4B lane 1). Treatment with BME caused VqmA-FLAG to
198 migrate more slowly, consistent with it being a reduced monomer (labeled R-Monomer;
199 Figure 4A and 4B lane 2). Administration of DPO drove formation of an additional
200 VqmA-FLAG species, corresponding in size to an oxidized dimer (labeled O-Dimer,
201 Figure 4A and 4B lane 3), but only under oxidizing (i.e., -BME) conditions (Figure 4B,
202 compare lanes 3 and 4). These results suggest that, under aerobic conditions, a fraction
203 of VqmA harbors an intra-molecular disulfide bond and DPO-bound VqmA forms an
204 inter-molecular disulfide bond. Under anaerobic conditions, the portion of VqmA
205 containing the intra-molecular disulfide bond decreased (Figure 4B compare lane 1 to

206 lane 5 and lane 5 to lane 6) while the DPO-dependent inter-molecular disulfide bonded
207 species was unaffected by the absence of oxygen (Figure 4A compare lane 3 to lane 7
208 and lane 7 to lane 8).

209 To garner additional evidence for the presence of an intra-molecular disulfide
210 bond(s) in the species designated VqmA O-monomer in Figure 4B, we treated samples
211 prepared from cells grown under +O_2 and -DPO conditions with methoxypolyethylene
212 glycol maleimide (m-MAL-PEG) (32). m-MAL-PEG alkylates reduced cysteine residues
213 and in so doing, confers an ~5 kDa molecular weight change for each alkylation event
214 (see schematic in Figure 4A). VqmA contains four cysteine residues, thus the fully
215 reduced protein would undergo 4 m-MAL-PEG events while if one intra-molecular
216 disulfide bond exists, only two cysteine residues could react. Following treatment, Apo-
217 VqmA-FLAG migrated primarily as two bands, corresponding to four (~40% of protein)
218 and two (~60% of protein) alkylation events (Figure 4C, compare lane 1 to lane 2),
219 confirming that while a portion of VqmA-FLAG is fully reduced *in vivo*, the majority of the
220 protein exists as an oxidized species containing one intra-molecular disulfide bond.

221 To determine the residues involved in VqmA disulfide linkages, we conducted
222 two experiments. First, we employed an *in vitro* thiol-trapping strategy based on
223 sequential reactions that modify accessible cysteine residues with two thiol-specific
224 reagents (Supplementary Figure 4A) (52). In the initial thiol-blocking step, purified 6His-
225 VqmA treated with diamide, a thiol-specific oxidant (30), was denatured and incubated
226 with chloroacetamide (CAA). CAA alkylates accessible cysteine residues (i.e., those not
227 involved in disulfide bonds), blocking them from further modification. The CAA treated
228 sample was next treated with TCEP, a reductant, enabling non-CAA labeled cysteines
229 to be reduced. These newly freed residues were labeled in the final alkylation step with
230 N-ethylmaleimide (NEM). The sample was then analyzed by mass spectrometry. The
231 logic is that if a particular cysteine residue was inaccessible to CAA due to disulfide
232 bonding, it would be preferentially labeled with NEM in the subsequent NEM
233 modification step. Thus, the NEM/CAA ratio would be >1. By contrast if a cysteine
234 residue was not involved in disulfide modification, it would be preferentially labeled with
235 CAA and have a NEM/CAA ratio < 1. The VqmA C48 and C63 residues had NEM/CAA
236 ratios of ~100 and ~10, respectively, suggesting both of these residues are involved in

237 disulfide-linkages (Supplementary Figure 4B). We were unable to obtain good coverage
238 of the C134 and C22 residues using this technique so we could not similarly assess
239 them.

240 Our second experiment to probe disulfide bonds in VqmA relied on mutagenesis.
241 We individually substituted an alanine residue for each cysteine residue in the p*vqmA-*
242 *FLAG* construct, introduced the plasmids into the Δ*vqmA* Δ*tdh V. cholerae* strain, and
243 repeated the analyses described in Figure 4C. We first consider the case of intra-
244 molecular disulfide bond formation under +O_2 -DPO conditions. In the mutant proteins,
245 following replacement of a cysteine residue with alanine, a maximum of three residues
246 can react with m-MAL-PEG in the fully reduced protein (Figure 4A, top). However, if an
247 intra-molecular disulfide bond is present, then only one cysteine residue can be
248 decorated with m-MAL-PEG. Figure 4C shows that the Apo-VqmA C22A and Apo-
249 VqmA C134A proteins each migrated as two bands, a result consistent with portions of
250 each protein harboring one and three m-MAL-PEG moieties (Figure 4C; compare lane 3
251 to lanes 2 and 1; and lane 6 to lanes 2 and 1). This result suggests that the fraction of
252 Apo-VqmA C22A and the fraction of Apo-VqmA C134A that exhibit one m-MAL-PEG
253 decoration harbor intra-molecular disulfide bonds. Apo-VqmA C48A and Apo-VqmA
254 C63A migrated largely as single bands at the region corresponding to three m-MAL-
255 PEG decorations (Figure 4C; compare lanes 4 and 5 to lane 2), suggesting that these
256 proteins exist as reduced species and are thus incapable of forming intra-molecular
257 disulfide bonds. Therefore, we conclude that in WT VqmA, an intra-molecular disulfide
258 bond is formed between cysteine residues 48-63.

259 Next, we consider inter-molecular disulfide bond formation under +O_2 +DPO
260 conditions, and under non-reducing conditions (i.e., -BME). Figure 4D shows that the
261 Holo-VqmA C22A, Holo-VqmA C48A, and Holo-VqmA C63A proteins migrated as
262 mixtures of oxidized monomers and oxidized dimers, while the Holo-VqmA C134A
263 protein migrated exclusively as an oxidized monomer (compare lanes 2-5 to lane 1).
264 These data suggest that in Holo-VqmA, there is a C134-C134 inter-molecular disulfide
265 linkage. We also constructed and assessed the double VqmA C63A C134A mutant
266 under +O_2 +m-MAL-PEG and +O_2 +DPO conditions. Figure 4C shows that under
267 aerobic conditions, all of the Apo-VqmA C63A C134A protein contains two m-MAL-PEG

268 decorations (compare lane 7 to lane 2), confirming that the two remaining cysteine
269 residues were accessible and that the protein is fully reduced. Figure 4D shows that
270 under aerobic conditions Holo-VqmA C63A C134A migrates entirely as a monomer
271 (compare lanes 6 to lane 1). Thus, Holo-VqmA C63A C134A is incapable of forming
272 both intra- and inter-molecular disulfide bonds.

273 Collectively our data suggest that: 1) VqmA forms disulfide bonds *in vivo* and *in*
274 *vitro*; 2) an intra-molecular disulfide bond is formed between VqmA C48-C63, and an
275 inter-molecular disulfide bond is made between C134-C134, and 3) disulfide bond
276 formation is influenced by both oxygen and DPO.

277

278 **VqmA activity is limited by the intra-molecular disulfide bond and enhanced by**
279 **the inter-molecular disulfide bond.** To explore the *in vivo* consequences of VqmA
280 disulfide bond formation on VqmA function, we tested whether the Apo- and Holo-
281 mutant VqmA proteins that are incapable of forming particular intra- and/or inter-
282 molecular disulfide bonds displayed altered abilities to activate target *vqmR*
283 transcription (see schematic in Supplementary Figure 5A). We introduced the *vqmA-*
284 *FLAG*, *vqmA C48A-FLAG* and the *vqmA C134A-FLAG* alleles onto the chromosome of
285 a *V. cholerae* Δ*tdh* strain carrying *vqmR-lacZ* and measured reporter activity following
286 aerobic growth +/- DPO. Our rationale was that WT VqmA forms both the C48-C63
287 intra-molecular bond and the C134-C134 inter-molecular bond. By contrast the VqmA
288 C48A variant is unable to form the C48-C63 intra-molecular bond and the VqmA C134A
289 variant is unable to form the C134-C134 inter-molecular bond (from Figure 4C and 4D).
290 Therefore, by comparing the activities of these three proteins, we could assess the
291 effect of individually eliminating each disulfide bond on VqmA activity. We likewise
292 made a strain carrying *vqmA C63A C134A-FLAG* on the chromosome to examine the
293 effect of simultaneous elimination of both disulfide bonds.

294 First we consider the case of Apo-VqmA. Apo-VqmA C48A and Apo-VqmA
295 C134A exhibited an ~2-fold and ~4-fold increase and decrease, respectively, in reporter
296 activity, relative to WT Apo-VqmA (Supplementary Figure S5B). Apo-VqmA C63A
297 C134A exhibited a ~3-fold increase in reporter activity relative to WT Apo-VqmA and a
298 ~10-fold increase in reporter activity relative to the strain carrying the Apo-VqmA C134A

299 single mutant (Supplementary Figure S5B). Thus, we conclude that the C48-C63 intra-
300 molecular disulfide bond limits transcriptional activity of Apo-VqmA.
301 Next, we consider the case for Holo-VqmA. In cultures supplemented with DPO,
302 *vqmR-lacZ* reporter activity increased ~20-30-fold, in a DPO-concentration-dependent
303 manner in the strain carrying WT Holo-VqmA relative to the strain with WT Apo-VqmA
304 (Supplementary Figure S5C). The strain carrying the VqmA C48A variant displayed a
305 further increase in DPO-dependent reporter activity relative to the WT-VqmA. However,
306 in strains harboring Holo-VqmA C134A and Holo-VqmA C63A C134A, only modest (3-
307 4-fold) responses to DPO occurred (Supplementary Figure S5C). Thus, the DPO-
308 responsive, C134-C134 inter-molecular disulfide-bond enhances VqmA transcriptional
309 activation activity.
310
311 **VqmA activity is differentially modulated by the cellular redox environment.** To
312 test whether VqmA activity is responsive to cellular redox, we supplemented the strains
313 carrying the different VqmA variants with DTT, a cell-permeable reductant. We
314 reasoned that if the absence of oxygen generates a reducing environment that prevents
315 the formation of a particular disulfide bond, addition of DTT would mimic this condition
316 by promoting a reducing cellular environment, including in the presence of oxygen. To
317 control for any potential DTT-induced changes in the levels of chromosomally
318 expressed *vqmA*, we introduced plasmids harboring arabinose inducible *vqmA-FLAG*,
319 *vqmA C134A-FLAG*, or *vqmA C63A C134A-FLAG* into the *V. cholerae* Δ*vqmA* Δ*tdh*
320 strain carrying *vqmR-lacZ* and measured reporter activity +/- DPO and +/- DTT.
321 In the absence of DTT, the Apo- and Holo- plasmid-borne VqmA variants
322 displayed reporter activities similar to when the variants were expressed from the
323 chromosome (plasmid-borne variants are in Figure 5A and 5B, compare the black bars
324 in each panel; for chromosomal variants, see Figure S5B and C). Treatment with DTT
325 increased reporter activity for WT Apo-VqmA and Apo-VqmA C134A but did not alter
326 the reporter activity in the strain carrying Apo-VqmA C63A C134A (Figure 5A, compare
327 black and gray bars for each strain). As a reminder, WT Apo-VqmA and Apo-VqmA
328 C134A form the C48-C63 intra-molecular disulfide bond, while the Apo-VqmA C63A
329 C134A protein does not. Thus, these data suggest that a reducing environment

330 interferes with formation of the C48-C63 intra-molecular disulfide bond, thereby
331 eliminating its negative effect on Apo-VqmA activity.
332 Regarding WT Holo-VqmA, reporter activity diminished by ~6-fold when DTT was
333 present in addition to DPO (Figure 5B; compare the first pair of black and gray bars). In
334 contrast, DTT supplementation did not significantly affect reporter activity in the strain
335 carrying Holo-VqmA C134A (Figure 5B; compare the second set of black and gray
336 bars), while ~3-fold lower activity was produced by the strain carrying Holo-VqmA C63A
337 C134A (Figure 5B; compare the third set of black and gray bars). Since the activity of
338 VqmA C134A was not affected by DTT supplementation, we conclude that the C134-
339 C134 inter-molecular bond does not form in a reducing environment, and without that
340 bond, Holo-VqmA transcriptional activity is diminished. Indeed, further emphasizing this
341 conclusion, following DTT administration, reporter activity declined 5-fold in the DPO
342 treated strain harboring arabinose inducible *vqmA C48A-FLAG* (Supplementary Figure
343 S5D).
344
345 **VqmA DNA binding capacity is differentially modulated by its redox environment.**
346 We suspected that the *in vivo* redox-dependent changes in VqmA disulfide bond
347 formation would have ramifications on VqmA DNA binding capability. To explore this
348 notion, we examined the ability of purified VqmA proteins to bind p*vqmR* promoter DNA.
349 First, to examine the role of the C48-C63 intra-molecular disulfide bond, we assessed
350 DNA binding for 6His-VqmA C134A treated with diamide (to enable disulfide bond
351 formation) or DTT (to prevent disulfide bond formation) (see Supplementary Figure 6).
352 Relative to the DTT treated protein, the diamide treated protein exhibited a 4-fold
353 reduction in DNA binding (Figure 5C; compare lanes 2-6 with lanes 7-11). This result
354 suggests that formation of the C48-C63 intra-molecular disulfide bond limits DNA
355 binding.
356 We investigated the role of the VqmA C134-C134 inter-molecular disulfide bond
357 on DNA binding by comparing the DNA binding capabilities of 6His-VqmA and 6His-
358 VqmA C134A. Diamide treated 6His-VqmA was approximately twice as potent at
359 binding DNA as was 6His-VqmA C134A [compare left halves of Figure 5C (VqmA
360 C134A) and Figure 5D (WT VqmA)], suggesting that the C134-C134 inter-molecular

361 disulfide bond promotes DNA binding. The DTT treated 6His-VqmA C134A and 6His-
362 VqmA proteins showed no difference in DNA binding capability [compare right halves of
363 Figure 5C (VqmA C134A) and Figure 5D (WT VqmA)]. Like 6His-VqmA C134A, DTT
364 treated 6His-VqmA was more proficient in DNA binding than diamide treated 6His-
365 VqmA, consistent with intra-molecular disulfide bond formation limiting DNA binding
366 (Figure 5D). Collectively, the data in Figures 4 and 5 suggest a model in which the
367 transcriptional and DNA binding activities of both Apo-VqmA and Holo-VqmA are
368 modulated by disulfide bond formation, the cytoplasmic redox environment, and by the
369 level of O_2 in the environment.
370
371 **Bile salts interfere with VqmA disulfide-bond formation and decrease VqmA**
372 **transcriptional activation activity.** Our above findings suggest that the VqmA-DPO
373 signal transduction pathway, which represses virulence factor production and biofilm
374 formation, is most highly active under anaerobic conditions. *V. cholerae* encounters
375 anaerobiosis in the human intestine. The paradox is that in the intestine, *V. cholerae* is
376 virulent and makes biofilms. We thus wondered if a possible host intestinal signal(s)
377 could modulate VqmA-DPO signaling, allowing infection to proceed under anaerobic
378 conditions. Bile salts, present in high concentrations in the human small intestine, can
379 alter the redox environment of bacterial cells and thereby affect disulfide bond formation
380 in cytoplasmic proteins (11). Thus, we were inspired to investigate whether bile salts
381 could abrogate VqmA-DPO transcriptional activation activity. We cultured the Δ*vqmA*
382 Δ*tdh V. cholerae* strain carrying the arabinose inducible *pvqmA-FLAG* construct and
383 *vqmR-lacZ* on the chromosome in the presence and absence of oxygen, bile, and DPO
384 and we measured reporter activity. Treatment with bile salts caused ~2- fold and ~10-
385 fold decreases in *vqmR-lacZ* reporter activity under +O_2 and -O_2 growth, respectively
386 (Figure 6A; first four bars). Supplementation with bile salts also decreased *vqmR-lacZ*
387 reporter activity in cultures supplied with DPO, again with the maximum effect observed
388 under -O_2 growth (Figure 6A; 5th bar onward). To test whether the presence of bile salts
389 affects VqmA disulfide bonds, we used analyses similar to those in Figure 4B.
390 Consistent with the *vqmR-lacZ* reporter activity, bile salts supplementation prevented
391 formation of O-dimers, both in the presence and absence of O_2, suggesting it interferes

392 with the Holo-VqmA C134-C134 inter-molecular disulfide bond (Figure 6B). We do not
393 know whether or not bile affects VqmA intra-molecular disulfide bond formation.
394
395 **Bile salts-mediated disruption of VqmA-DPO-driven signal transduction promotes**
396 ***V. cholerae* virulence**. In *V. cholerae*, VqmA-DPO-directed production of VqmR results
397 in decreased expression of genes involved in biofilm formation and virulence factor
398 expression, including *vpsL* and *tcpA*, respectively (46, 47). VpsL is required to
399 synthesize *V. cholerae* exopolysaccharide, an essential component of the biofilm matrix,
400 and TcpA is a virulence factor required for *V. cholerae* to colonize the human small
401 intestine (17, 57). Our finding that supplementation with bile salts inhibited VqmA-DPO
402 function and that the effect of bile salts-mediated inhibition occurred primarily in the
403 absence of oxygen, led us to predict that the repression of *vpsL* and *tcpA* expression
404 would also be maximally disrupted following bile salts supplementation in the absence
405 of oxygen. We measured transcript levels of *vpsL* and *tcpA* in the WT and Δ*vqmA*
406 strains following exposure to 25 μM DPO, bile salts, deprivation of oxygen, or
407 combinations of the three treatments.
408 In WT *V. cholerae*, bile salts supplementation modestly increased *vpsL* and *tcpA*
409 transcript levels (~3- and ~2-fold, respectively) however, only under -O_2 -DPO
410 conditions (Supplementary Figure 7 and Figure 6C). These data suggest that bile salts
411 induce genes required for biofilm formation and virulence in the absence of oxygen and
412 Holo-VqmA can override the effect of bile. Transcript levels for both *vpsL* and *tcpA*,
413 under -O_2 -DPO conditions were further increased in the Δ*vqmA* strain treated with bile
414 salts (~6- and ~3-fold, respectively). We interpret this result to mean that bile salts also
415 induce an increase in *vpsL* and *tcpA* expression through a pathway that does not
416 involve VqmA. However, because the major effect of bile salts occurs only in the Δ*vqmA*
417 strain, we conclude that this additional pathway is epistatic to VqmA in the control of
418 *vpsL* and *tcpA*.
419 We tested whether the above changes in gene expression translated into
420 alterations in *V. cholerae* pathogenicity by assaying whether bile salts affected
421 cytotoxicity of *V. cholerae* in co-culture with human Caco-2 intestinal cells. We
422 generated differentiated monolayers of Caco-2 cells and co-cultured them with either

423 WT or Δ*vqmA V. cholerae* in the presence and absence of bile salts. The presence of
424 bile salts, increased *V. cholerae*-mediated cytotoxicity to Caco-2 cells with the Δ*vqmA*
425 strain driving twice as much killing as WT *V. cholerae* (Figure 6D). Collectively, our data
426 suggest that bile salts induce increased *V. cholerae* virulence when bacteria are
427 deprived of oxygen, part of the bile salt effect is exerted via interference with the VqmA-
428 DPO-VqmR QS circuit, and the presence of VqmA limits the ability of bile salts to affect
429 target gene expression.
430
431 **Discussion:**
432 The diversity of environments that *V. cholerae* inhabits, from the ocean to marine
433 organisms to the human stomach to the human intestine, necessitates that the
434 bacterium rapidly perceives changes in its external environment and appropriately
435 tailors its gene expression programs. Our current study reveals that *V. cholerae* alters
436 both which AIs are produced and the functioning of the VqmA-DPO-VqmR QS circuit in
437 response to its environment. To our knowledge, these findings represent the first
438 dissection of QS activity in the absence of oxygen in a facultative aerobic bacterium. We
439 find that 1) the amounts of two AIs (CAI-1 and DPO) produced is dictated by oxygen
440 levels; 2) a single QS protein (VqmA) is capable of integrating information from three
441 sources (AI, oxygen, bile salts); and 3) two disulfide bonds in a QS receptor (VqmA)
442 antagonize one another with respect to their effects on protein activity, thereby aiding in
443 perception and response to changes in cellular redox.
444 The benefit(s) of producing and detecting multiple QS AIs has long been
445 mysterious with respect to *V. cholerae* biology. Evidence suggests that each AI conveys
446 specific information into the cell: CAI-1 measures the abundance of vibrios (kin) and AI-
447 2 and DPO measure the level of non-vibrio (non-kin) in the vicinity (5, 46, 47). Our
448 finding that CAI-1 is not produced in the absence of oxygen suggests that CAI-1 may
449 also convey information about the external environment. Strains lacking the ability to
450 synthesize CAI-1 display reduced survival in seawater and following challenge with
451 oxidative stress (25). Thus, we propose that CAI-1 could drive the expression of genes
452 required for the aerobic segment of the *V. cholerae* lifecycle and we are now testing this
453 idea. The fact that CAI-1 is not produced under anoxia suggests that *V. cholerae* cannot

454 take a census of kin in the absence of oxygen. Either kin counting is dispensable under
455 anoxia or, perhaps, another molecule(s)/mechanism performs this function. By contrast,
456 at a minimum based on sequencing data, thousands of bacterial species, including
457 those found in the human microbiota, can synthesize AI-2, the AI used for inter-species
458 communication (49). We found that AI-2 is synthesized in the absence of oxygen.
459 Perhaps measurement of the abundance of non-kin bacteria is of paramount
460 importance in densely populated niches containing complex bacterial consortia.
461 Biosynthesis of both AI-2 and CAI-1 requires *S*-adenosylmethionine (SAM), an
462 abundant metabolite that is crucial for methylation reactions (8, 28, 54). Thus, another
463 possibility is that in *V. cholerae*, during periods of SAM limitation, CAI-1 production is
464 curbed as a means of sparing SAM for other uses. Continued AI-2 production could
465 suffice for QS-mediated cell-density tracking. Moreover, when SAM is used to produce
466 AI-2, but not CAI-1, SAM is regenerated via downstream reactions (54, 61). Thus,
467 making AI-2 from SAM would not deplete the SAM reservoir.

468 Oxygen is a terminal electron acceptor and therefore a critical substrate for
469 bacterial growth. The human intestine is devoid of oxygen, and invading bacteria, such
470 as *V. cholerae* that normally inhabit the relatively oxygenated marine environment, need
471 to alter their physiology to survive. With the exception of a handful of studies (31, 33,
472 35), the molecular mechanisms by which *V. cholerae* perceives the absence of oxygen,
473 and translates this information into changes in gene expression, are unexplored. Here,
474 we demonstrate that, in the presence of O_2, Apo-VqmA forms a C48-C63 intra-
475 molecular disulfide bond that restricts the ability of the protein to bind DNA. Formation of
476 this bond is inhibited in the absence of oxygen or following supplementation of aerobic
477 cells with a reductant, that, analogous to the absence of oxygen, generates a reducing
478 environment. Thus, we propose that by interacting with the cell's redox environment,
479 VqmA provides *V. cholerae* a mechanism to monitor oxygen levels (Figure 7A). In this
480 context, we note that anaerobiosis causes a ~7-fold increase in Apo-VqmA-dependent
481 p*vqmR-lacZ* reporter activity (Figure 3B). By contrast, DTT supplementation under
482 aerobic conditions causes only an ~3-fold increase in Apo-VqmA activity while the
483 activity of Apo-VqmA C63A C134A, that lacks both disulfide bonds, is unchanged
484 (Figure 5A). One interpretation of these data is that Apo-VqmA is responsive to

485 additional oxygen-dependent stimuli that are not mimicked by DTT or by the inability to
486 make disulfide bonds. We are currently testing this possibility.

487 With respect to DPO-bound VqmA we found that Holo-VqmA forms a C134-C134
488 inter-molecular disulfide bond. Our data expand on a recent structural study of VqmA in
489 which the crystal structure revealed the C134-C134 disulfide bond in Holo-VqmA. The
490 authors predicted that the C134-C134 bond could interfere with VqmA DNA binding
491 (62, 63). However, the role of the disulfide bond on VqmA activity was not
492 experimentally investigated in that earlier work (63). Here, we show that the C134-C134
493 bond is largely absent in Apo-VqmA while, upon binding DPO, ~40-50% of Holo-VqmA
494 undergoes inter-molecular C134-C134 disulfide bond formation, and moreover, this
495 bond promotes Holo-VqmA activation of transcription (Figure 4B and Figure 5). We do
496 not understand why the conclusion one naturally comes to from the crystal structure
497 does not match the experimental data. We do note that the C134 residue is located in a
498 flexible loop region. Thus, one possibility is that, in the static crystal, the loop region is
499 spatially constrained and does not reflect dynamic structures that VqmA adopts in
500 solution. This notion awaits experimental testing.

501 Our results show formation of the C134-C134 bond is not modulated by oxygen
502 levels but is inhibited by the reductant DTT. The absence of oxygen imposes a mildly
503 reducing environment on cells, while the presence of DTT imposes reductive stress (42,
504 58), suggesting that the C134-C134 inter-molecular VqmA disulfide bond may allow *V.*
505 *cholerae* to monitor reductive stress. Under *in vitro* conditions, the negative effect
506 exerted by the C48-C63 intra-molecular disulfide bond on DNA binding was more
507 significant than the positive effect exerted by the C134-C134 inter-molecular disulfide
508 bond. This result contrasts with our *in vivo* data (Figure 5B), in which the inter-molecular
509 disulfide bond has the most pronounced effect on WT VqmA activity. One explanation
510 that we are now exploring is that *in vivo*, additional factors modulate the activity of WT
511 VqmA containing the inter-molecular disulfide bond. Collectively, we suggest a model in
512 which cycling between multiple redox states, namely Oxidized-Apo-VqmA, Reduced-
513 Apo-VqmA, Oxidized-Holo-VqmA, and Reduced-Holo-VqmA, enables *V. cholerae* to
514 tune its QS-controlled collective behaviors to a range of redox states (Figure 7B). There
515 exist examples of individual disulfide bonds restricting or enhancing the activity of

516 transcription factors (7, 10, 67). To our knowledge, however, this is the first example in
517 which the same protein simultaneously uses two different disulfide bonds to modulate
518 activity.

519 Bile is an abundant compound in the human small intestine that is well known to
520 alter virulence in *V. cholerae* and other enteric pathogens such as *Salmonella*
521 *typhimurium* and *Shigella flexneri* (19, 43). Bile is a heterogeneous mixture of molecules
522 and studies have largely focused on defining the roles of individual components in
523 bacterial physiology. Intriguingly, the individual components can drive opposing effects.
524 In *V. cholerae*, bile fatty acids repress while the bile salt taurocholate induces virulence
525 (6, 9, 23, 36, 50, 65). In our current study, we elected to use a mixture of bile salts
526 reasoning that this strategy would more closely approximate what *V. cholerae*
527 encounters *in vivo*. Our data suggest that bile salts disrupt the formation of the VqmA
528 C134-C134 inter-molecular disulfide bond. We do not know the mechanism by which
529 this occurs. However, previous studies show that bile salts, specifically cholic acid
530 (CHO) and deoxycholic acid (DOC), interfere with redox homeostasis in *Escherichia coli*
531 by shifting the cellular environment to an oxidizing one and fostering disulfide bond
532 formation in cytosolic proteins (11). In the context of our work, since VqmA inter-
533 molecular disulfide bond formation is disrupted, we propose that application of a bile
534 salts mixture to *V. cholerae* causes reductive stress. Consistent with this idea,
535 taurocholate binds to and inhibits DsbA, a protein required for the introduction of
536 disulfide bonds in periplasmic proteins (64). We currently do not know whether
537 incubation of *V. cholerae* with CHO and DOC, rather than a bile salts mixture, would
538 drive phenotypes mimicking those observed in *E. coli*.

539 What advantage does *V. cholerae* accrue by using the regulatory program
540 uncovered in our study? We propose that *V. cholerae* uses the different blends of AIs it
541 encounters along with environmental modulation of VqmA activity to gauge its changing
542 locations in the host. Thus, VqmA functions rather like a “GPS-device”. In response to
543 the information obtained about its micro-environment through VqmA, *V. cholerae* can
544 appropriately tune its gene expression in space and time. We say this because, prior to
545 entry into the small intestine (the site of cholera disease), *V. cholerae* will encounter
546 oxygen limitation in the stomach. However, premature expression of virulence genes in

547 the stomach, in the face of low pH and antimicrobial peptides would be unproductive
548 and, moreover, divert energy from combating host defense systems. Thus, increased
549 VqmA activity, due to enhanced accumulation of DPO under anoxia coupled with
550 formation of the C134-C134 inter-molecular disulfide bond and suppression of formation
551 of the activity-dampening intra-molecular disulfide bond, will increase production of
552 VqmR and, in turn, repress expression of genes involved in biofilm formation and
553 virulence. Anoxia and the concurrent presence of bile, encountered upon entry into the
554 host duodenum (upper region of the small intestine), may provide a spatially relevant
555 signal to alert *V. cholerae* to begin to express virulence genes. In this case, bile salts-
556 mediated inhibition of VqmA activity due to prevention of formation of the inter-
557 molecular disulfide bond will decrease VqmR production and, in turn, enhance
558 expression of genes involved in biofilm formation and virulence. The combined use of
559 bile salts and anoxia to decrease and increase VqmA activity, respectively, is also
560 noteworthy because, as *V. cholerae* proceeds further through the intestinal tract,
561 concentrations of bile salts decrease near the ileum (lower portion of the small
562 intestine), where ~95% of bile salts are reabsorbed, and they reach a minimum in the
563 large intestine. By contrast, anoxia is maintained throughout the intestinal tract. During
564 successful infection, *V. cholerae* cell numbers increase as disease progresses.
565 Accumulation of DPO should track with increasing cell density. Thus, it is possible that
566 late in infection, *V. cholerae* resides in a high DPO, anoxic environment lacking bile
567 salts, conditions enabling re-engagement of the VqmA-VqmR-DPO circuit, termination
568 of virulence factor production, and expulsion from the host. In this context, we also note
569 that DPO production by *V. cholerae* requires threonine as a substrate. Mucin is a major
570 constituent of the intestinal tract and is composed of ~35% threonine (26). Intriguingly,
571 both the stomach and large intestine, locations where *V. cholerae* typically does not
572 reside, contain more mucus secreting glands and mucus layers than does the small
573 intestine (26). Thus, it is likely that enhanced access to mucus-derived threonine in the
574 large intestine allows *V. cholerae* to increase DPO production. Again, high DPO levels
575 repress virulence and biofilm formation. Thus, increased DPO production in the large
576 intestine would foster *V. cholerae* departure from the host. We speculate that, in
577 addition to oxygen and bile salts, the presence of mucus/threonine/the ability to

578 synthesize DPO is also leveraged by *V. cholerae* as an additional spatial cue to
579 optimize host dispersal timing.
580
581 **Materials and Methods:**
582
583 **Materials:** iProof DNA polymerase was purchased from Biorad. Gel purification,
584 plasmid-preparation, RNA-preparation (RNeasy), RNA-Protect reagents, qRT-PCR kits,
585 and deoxynucleoside triphosphates were purchased from Qiagen. Antibodies were
586 purchased from Sigma. Chitin flakes were supplied by Alfa Aesar. Instant Ocean (IO)
587 Sea Salts came from from Tetra Fish. Bile salts were purchased from Fluka.
588
589 **Bacterial growth:** *E. coli* Top10 was used for cloning, *E. coli* S17-1 λ*pir* was used for
590 conjugations, and *E. coli* BL21 (DE3) was used for protein purification. *V. cholerae* and
591 *E. coli* strains were grown in LB medium or in M9 minimal medium with glucose at 37°C,
592 with shaking. When required, media were supplemented with streptomycin, 500 μg/mL;
593 kanamycin 50 μg/mL; spectinomycin, 200 μg/mL, polymyxin B, 50 μg/mL; and
594 chloramphenicol, 1 μg/mL. For bioluminescence assays, *V. cholerae* strains were
595 cultured in SOC medium supplemented with tetracycline, and for AI-2 measurements,
596 with boric acid (20 μM). Unless otherwise indicated, bile salts were supplemented at
597 0.5% v/v and DPO at 25 μM. Where indicated, oxygen deprivation was achieved as
598 follows: a) medium was sparged prior to use for at least 20 min with nitrogen gas; b)
599 medium was incubated overnight with constant stirring inside a COY anaerobic
600 chamber equipped with a catalyst to scavenge oxygen. For both (a) and (b), subsequent
601 steps were conducted inside the COY anaerobic chamber and c) exponentially growing
602 cells were transferred into capped microcentrifuge tubes with a headspace to volume
603 ratio (HV ratio) of zero and anaerobiosis was verified by the addition of 0.001%
604 resazurin to control tubes, as described previously (18, 37). Micro-aerobiosis was
605 achieved at ~10 min post-shift and anaerobiosis by ~15-18 min post-shift under these
606 conditions, consistent with previous observations (18). Experiments presented in Figure
607 1 were conducted using strategy (a) and (b). Experiments in later sections used strategy
608 (c). In control experiments, we verified that our data were not altered due to differences

609 in growth in the presence or absence of oxygen (see Supplemental Figure 1B).
610 Experiments in Figure 1 were performed following *V. cholerae* growth in LB medium,
611 which supports production of CAI-1, AI-2, and DPO. When grown in M9 minimal
612 medium (Figures 3-6), *V. cholerae* does not produce DPO because supplementation
613 with threonine is required (47). Finally, we note that *V. cholerae* produces ~1-2 μM
614 DPO. In *in vivo* experiments, we treated cells with DPO at levels from 0-100 μM and in
615 *in vitro* experiments we used the fixed concentration of 25 μM. The goal was to assay
616 DPO responses from far below to well above the EC_{50} *in vivo*, and in the *in vitro*
617 experiments, to ensure that VqmA was always saturated with ligand.
618
619 **Strain construction:**
620 ***Chromosomal alterations****: V. cholerae* strains were constructed using natural-
621 transformation mediated multiplexed-genome-editing (MuGENT) (12, 13). Unless
622 otherwise stated, chromosomal DNA from *V. cholerae* C6706 Sm^R was used as a
623 template for PCR reactions. DNA fragments containing ~3 kb of homology to the
624 upstream and downstream regions of the desired chromosomal region were generated
625 using PCR. When necessary, SOE PCR was used to combine multiple fragments of
626 DNA, in which each fragment typically contained ~27-30 bp of overhang homology (12,
627 13). Antibiotic resistance cassettes, to facilitate selection of transformants following the
628 MuGENT step, were designed to integrate at a neutral locus (*vc1807*) and were gifts
629 from the Dalia group (Indiana University) (12, 13). *V. cholerae* cultures for use in natural
630 transformations were prepared by inoculating 1 mL liquid LB medium from freezer
631 stocks and growing the cells to OD_{600}~1. Cells were pelleted at maximum speed in a
632 micro-centrifuge and resuspended at the original volume in 1X IO Sea Salts (7 g/L).
633 Competence was induced by combining a 75 μL aliquot of the cell suspension with 900
634 μL of a chitin IO mixture (8 g/L chitin), and the preparation was incubated overnight at
635 30°C. The next day, these mixtures were supplemented with one (or multiple) PCR-
636 amplified linear DNA fragment(s) of interest, as well as DNA encoding an antibiotic
637 resistance cassette (12, 13). These mixtures were incubated overnight at 30°C, followed
638 by vortex for 10 min. Next, 150 μL of the suspension was plated onto solid LB medium
639 containing the appropriate antibiotics followed by overnight incubation at 30°C.

640 Resulting transformants were passaged three times on solid LB medium with antibiotics
641 for purification. Genomic DNA from recombinant strains was used as a template for
642 PCR to generate DNA fragments for future co-transformation, when necessary.
643
644 Site-directed mutations in *vqmA* were constructed by incorporating the desired
645 alteration into forward or reverse PCR primers and generating DNA fragments with
646 homology to DNA flanking chromosomal *vqmA*. These fragments were transformed, as
647 described above, into a strain carrying *vmqA*::*kan* and the *vqmR-lacZ* transcriptional
648 reporter integrated onto the chromosome. Clones were selected by screening for loss of
649 kanamycin resistance and/or by assessment of positive LacZ activity when plated on
650 agar containing 50 µg/mL X-gal.
651
652 ***Plasmid constructions****:* DNA cloned into the pBAD-pEVS or pEVS plasmids was
653 assembled using enzyme-free XthA-dependent *in vivo* recombination cloning, as
654 previously described (3, 41). Briefly, linear insert DNA fragments containing 30 base
655 pairs of overlapping homology were generated using PCR. The plasmid backbone was
656 likewise linearized by PCR-amplification. All DNA fragments were gel purified and
657 eluted in ddH_2O. Thereafter, 80 ng of the backbone and 240 ng of each insert DNA
658 fragment were combined, incubated for 1 h at room temperature followed by
659 transformation and clone recovery in chemically-competent Top10 *E. coli* cells.
660 Constructs in the pET15b backbone were assembled using traditional restriction-
661 enzyme cloning using primers and protocols described earlier (46).
662
663 **Assessing protein abundance and formation of disulfide bonds:** Strains cultured
664 overnight in LB medium (~16-18 h) were diluted into fresh M9 minimal medium, with
665 antibiotics, as necessary, to a final OD_{600}=0.004. When assessing levels of VqmA-FLAG
666 produced from the chromosomally-integrated *vqmA-FLAG* construct, strains were
667 cultured to OD_{600}~0.3 (~4 h of growth) and cells were harvested by centrifugation. For
668 strains requiring induction of protein expression, 0.2% arabinose was added to the
669 culture medium at 4 h post-inoculation and growth was continued for an additional 1 h at
670 which point the cultures were divided and portions were supplemented with 25 µM DPO

671 and/or 0.5% bile salts and/or deprived of oxygen. Treatments were continued for
672 another 1 h after which cells were harvested by centrifugation at 13,000 rpm and the
673 pellets were immediately frozen at -80°C until use.
674
675 **Immunoblotting:** Cells were resuspended in ice-cold PBS and diluted to a final
676 OD_{600}=7 for protein produced from the chromosome or to OD_{600}=3.5 for protein
677 produced from a plasmid, in a volume of 20 µL. The cells were lysed by addition of 5 µL
678 Bug Buster (Novagen) supplemented with 1 µg lysozyme, and 25 U/mL benzonase.
679 Samples were combined with SDS-PAGE buffer in the presence or absence of BME
680 (100 mM), boiled for 20 min, and proteins separated on 4–20% Mini-Protein TGX gels
681 (Biorad). Proteins were transferred to PVDF membranes (Bio-Rad) for 1 h at 4°C at 100
682 V. Membranes were blocked overnight in PBST (1X PBS, 0.03% Tween-20)
683 supplemented with 5% milk, washed 5 times with PBST, and incubated for 40 min with
684 1:5000 dilution of monoclonal Anti-FLAG-Peroxidase antibody (Sigma) in PBST. The
685 membranes were subsequently washed another five times with PBST. FLAG epitope-
686 tagged protein levels were visualized using the Amersham ECL western blotting
687 detection reagent (GE Healthcare). Thereafter, the antibody was removed by 2 serial
688 incubations in stripping buffer (15 g/L glycine, 1 g/L SDS, 10 mL/L Tween-20, pH 2.2)
689 for 5 min each. The membrane was re-equilibrated by 4 washes in PBST, 20 min each,
690 and used to detect the abundance of the loading control, RNA Polymerase α. Washes
691 and incubations as described above were performed to enable antibody binding and
692 removal of excess. The primary antibody, anti-*E. coli* RNA Polymerase α (Biolegend),
693 and the secondary antibody, anti-mouse IgG HRP conjugate antibody (Promega), were
694 both used at a 1:10,000 dilutions. In all cases, protein levels were quantified using
695 Image J software.
696
697 **Protein purification:** pET15b plasmids encoding 6XHis-VqmA were mobilized into
698 Δ*tdh E. coli* BL21 DE3. Strains were cultured for protein production as described
699 previously (22, 46). Cells were harvested by centrifugation and pellets were
700 resuspended in 1/100 volume of lysis buffer (50 mM Tris, 150 mM NaCl, pH 7.5
701 containing 0.5 mg/mL lysozyme, 1X protease inhibitor, and benzonase) for five min

702 followed by the addition of an equal volume of Bugbuster Reagent (Novagen). The cell
703 lysate was clarified by centrifugation at 13,000 rpm and protein was purified using Ni-
704 NTA superflow resin (Qiagen), according to the manufacturer's recommendations for a
705 centrifugation-based protocol, except that the loading and wash buffers all contained 1-
706 5 mM imidazole to decrease non-specific protein binding. The protein was eluted from
707 the resin using 300 mM imidazole and thereafter dialyzed twice against 50 mM Tris, 150
708 mM NaCl, pH 7.5, using a Slide-A-Lyzer module (Thermo Fisher). When necessary,
709 buffers were amended with 5 mM DTT. To purify Holo-VqmA, buffers were
710 supplemented with 100 μM DPO.
711
712 **Electromobility gel shift assays (EMSA):** The DNA corresponding to the promoter
713 region of *vqmR*, ~100 base pairs, was amplified using *V. cholerae* genomic DNA as a
714 template. Where mentioned, protein was pre-treated in binding buffer with 10-fold molar
715 excess of DTT or diamide in order to reduce or oxidize the protein, respectively. To
716 initiate EMSA assays, 0.2-3.5 μM protein was combined with 30 ng probe DNA in
717 binding buffer (50 mM Tris-HCl pH 8, 150 mM NaCl). Reactions were allowed to
718 proceed at RT for 15 min. Samples were separated on a Novex 6% DNA Retardation
719 Gel (Thermo) by electrophoresis in 1X TBE at 100 V. Gels were subsequently incubated
720 with Sybr Green reagent, diluted in 1X TBE at RT for 25 min, washed with five
721 successive rounds of ddH_2O, and imaged using an ImageQuant LAS 4000 imager and
722 the Sybr Green channel setting.
723
724 **Analysis of relative AI levels in conditioned growth medium following aerobic or**
725 **anaerobic growth:** *V. cholerae* strains were cultured overnight in LB medium (~16-18
726 h), diluted into fresh aerobic or anaerobic LB medium to a final OD_{600}=0.004. The
727 cultures were incubated at 37°C for an additional ~6 h with shaking. The cells were
728 removed by centrifugation at 13,000 rpm and the spent medium filtered through 0.2 μm
729 filters. 20% (v/v) 5X LB was added to the spent medium preparations (hereafter
730 designated as reconditioned spent medium). Negative controls consisted of spent
731 medium prepared from strains incapable of synthesizing CAI-1, AI-2, and DPO.
732 Subsequently, reconditioned spent medium was combined with *V. cholerae* reporter

733 strains expressing only a single QS receptor that, therefore detect only one AI. In the
734 case of CAI-1 and AI-2 detection, the reporter strains carried a plasmid encoding the *V.*
735 *harvyei luxCDABE* (luciferase) operon (39). For DPO detection, the reporter strain
736 possessed a p*vqmR-lux* (luciferase) fusion on the chromosome in place of the native
737 *lacZ* locus (22). Genotypes are provided in Table S1. The reporter strains and
738 reconditioned spent medium preparations were combined to a final volume of 150 µL in
739 wells of 96-well plates, covered with Breathe-Easy Film, and incubated at 30°C with
740 shaking for 2.5-4 h. Finally, bioluminescence and OD_{600} values were recorded. Relative
741 light units (RLU) were defined as light production (counts per minute) divided by OD_{600}.
742 Normalized RLUs were obtained by subtraction of the RLU values obtained from the
743 negative controls.
744
745 **Beta-galactosidase assays:** *V. cholerae* strains cultured overnight in LB medium were
746 diluted into fresh M9 medium to a final OD_{600}=0.004 and thereafter cultured to
747 OD_{600}~0.3 (~4 h). The cultures were held on ice prior to assay or subjected to further
748 treatments, as described below. For strains requiring inducible protein expression,
749 0.01% arabinose was added to the culture medium at 4 h post-inoculation and growth
750 was continued for an additional 1 h. In all cases, cultures were divided into aliquots and
751 individual portions were supplemented with 25 µM DPO and/or 0.5% bile salts and/or
752 deprived of oxygen. Cells were cultured for an additional 1 h and then held on ice prior
753 to assay. To assess the effect of reductant, at 2 h post-inoculation, the cultures were
754 supplemented with 300 µM DTT. Cells were cultured for another 2 h to allow DTT
755 permeation, before *vqmA* expression was induced by the addition of arabinose.
756 Subsequent treatments were as above. LacZ activity assays were carried out as
757 follows: cells were combined 1:1 (v/v) with Bugbuster Reagent for 20 min. The assay
758 was initiated by combining 20 µL of the cell/Bugbuster mixture with 140 µL of assay
759 buffer (80% Bugbuster, 10% 10X PBS, 1 mM $MgSO_4$, 10 µg/mL lysozyme, benzonase
760 (0.05% v/v), β-mercaptoethanol (0.1% v/v), 67 µg/mL fluorescein-di-β-D-
761 galactopyranoside). Changes in fluorescence were captured using the GFP channel on
762 a Synergy Neo2 HTS Multi-Mode Microplate Reader. Activity units were defined as the
763 change in fluorescence/minute/ OD_{600} of the culture at the point of harvest.

764

765 **RNA isolation and quantitative RT-PCR.** Strains cultured overnight in LB were diluted
766 into fresh M9 minimal medium to a final OD_{600}=0.004. Next, the strains were grown to
767 OD_{600}~0.3 (~4 h post-inoculation) with shaking at 37°C at which point the cultures were
768 divided into portions that were supplemented with 25 μM DPO and/or 0.5% bile salts
769 and/or deprived of oxygen. Treatments were continued for another 1 h, the cells were
770 harvested and treated for 15 min at room temperature with RNAProtect reagent, as per
771 the manufacturer's instructions. RNA was isolated using the RNeasy kit (Qiagen) and 2
772 μg of total RNA was depleted of contaminating DNA using TurboDNase (Applied
773 Biosystems), using the manufacturer's recommended protocol. 500 ng of the resulting
774 total RNA was used to construct cDNA libraries using SuperScript III Reverse
775 Transcriptase (Invitrogen). q-PCR was conducted using the PerfeCTa SYBR Green
776 FastMix Low ROX (Quanta Biociences) reagent.

777

778 **Caco-2 culture and co-culture with bile salts and *V. cholerae*.** The HTB37 cell line
779 was obtained from ATCC and thereafter cultured and passaged in EMEM (ATCC)
780 supplemented with an 10% FBS (Thermo Fisher), 2 mM glutamine (Thermo Fisher), 1X
781 Penstrep (Thermo Fisher) and 2.5 μg/mL plasmomycin (Invitrogen), as per ATTC
782 recommendations. Prior to co-culture, Caco-2 cells were seeded at 0.32 cm^2 into a
783 tissue culture treated 96-well plate in EMEM medium, as above, except that the 2 mM
784 glutamine was not included. The cells were cultured to confluency, the medium was
785 removed by aspiration, and the cells were washed with Earle's balanced salt solution
786 followed by the addition of EMEM medium containing 25 μM DPO, but lacking
787 antibiotics/glutamine/FBS. At time zero, *V. cholerae*, grown as described below, was
788 added, at an MOI of 10 and with 0.05% bile salts. Following co-culture for 3.5 h, the
789 medium and the bacteria were removed by aspiration, the wells were washed with
790 Earle's balanced salt solution, and Caco-2 cell viability was assessed using the neutral
791 red assay (51). For co-culture with Caco-2 cells, *V. cholerae* WT and Δ*vqmA* strains
792 were cultured overnight under static conditions in AKI medium containing 25 μM DPO in
793 tubes with an HV ratio of zero at 37°C. The next day, the cells were decanted into glass

794 tubes and cultured with vigrous shaking for 1 h. Subsequently, the cultures were diluted
795 with PBS to the appropriate density and added to the Caco-2 cells.
796
797 **Acknowledgements:** We thank the Donia lab for generously allowing us to use their
798 anaerobic chamber. We thank Dr. Ankur Dalia for the gift of protocols, strains, and
799 reagents to facilitate MuGENT cloning. We thank Dr. Tharan Srikumar, Saw Kyin, and
800 Henry Shwe for help with mass spectroscopy experiments. This work was supported by
801 the Howard Hughes Medical Institute, National Science foundation Grant MCB-
802 1713731, and NIH Grant 5R37GM065859 to B.L.B. A.A.M is a Howard Hughes Medical
803 Institute Fellow of the Life Sciences Research Institute.
804
805 **Competing interests:** The authors have no competing interests to declare.
806

807 **Figures and Figure Legends:**

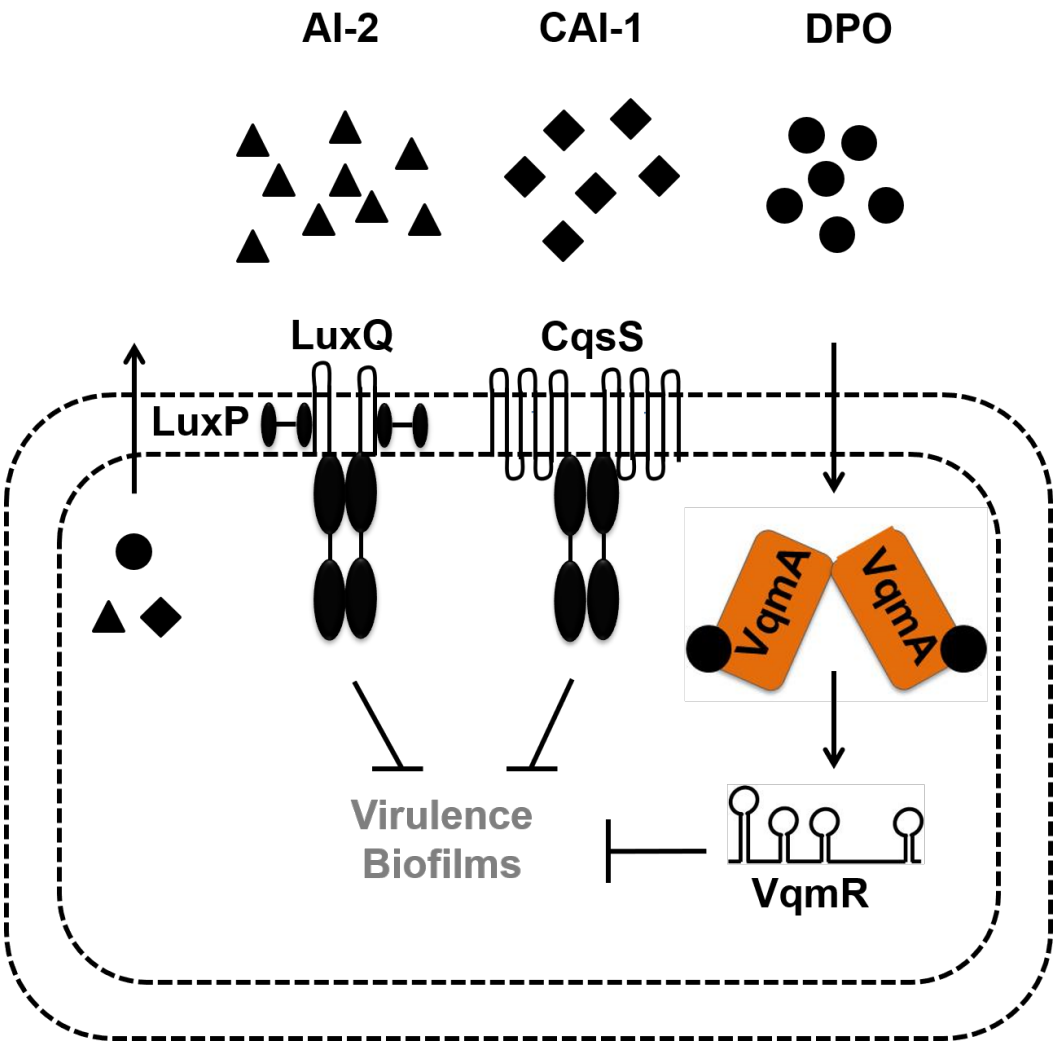

808

809 **Figure 1.** Simplified *V. cholerae* quorum-sensing pathways. See text for details.

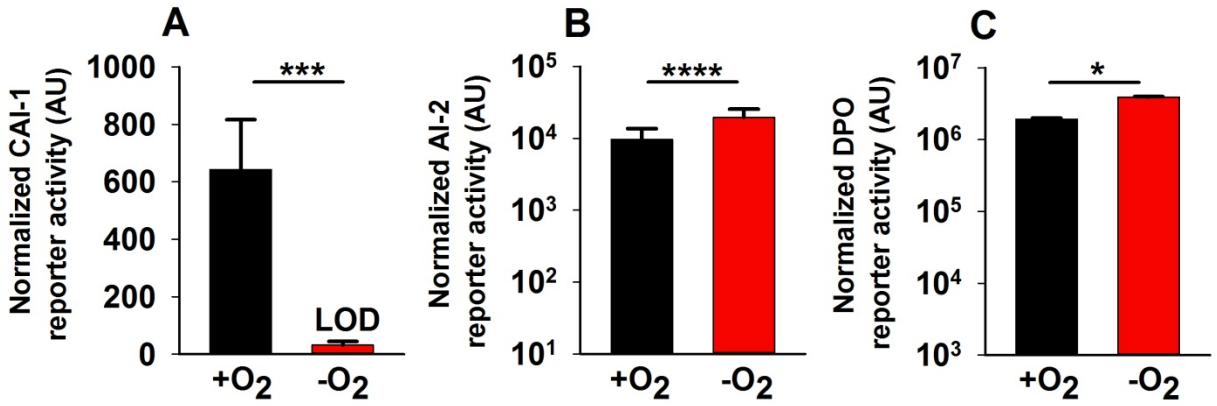

Figure 2. Oxygen deprivation modulates *V. cholerae* AI production. **(A)** 80%, **(B)** 25%, or **(C)** 30% cell-free culture fluids prepared from WT *V. cholerae* grown in the presence or absence of O_2 were provided to *V. cholerae* reporter strains that produce bioluminescence in response to exogenous **(A)** CAI-1, **(B)** AI-2, or **(C)** DPO. Data represent the average values of biological replicates (*n*=3) and error bars represent SD. Statistical significance was calculated using a two-tailed Student's t-test. Asterisks as follows: $p<0.05$, *** denotes $p<0.001$, and **** denotes $p<0.0001$.

819

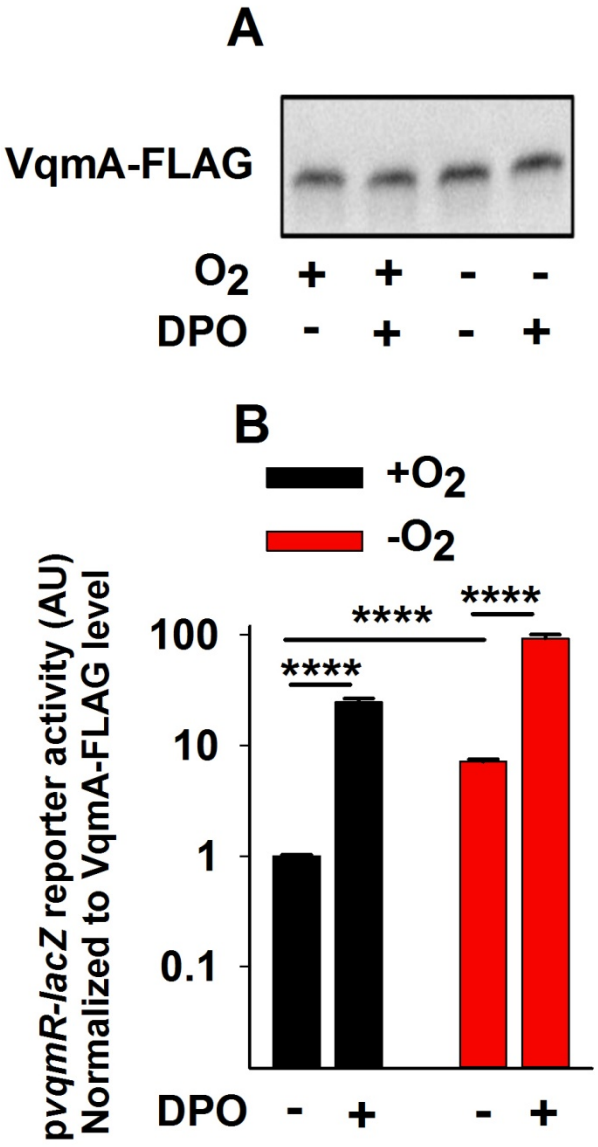

820

821

822 **Figure 3**. Apo- and Holo-VqmA activities are enhanced in the absence of oxygen. **(A)**
823 Western blot showing VqmA-FLAG abundance in the Δ*vqmA* Δ*tdh V. cholerae* carrying
824 p*vqmA-FLAG* and treated as shown for 1 h. DPO was supplied at 25 μM. **(B)**
825 Transcriptional activity for the p*vqmR-lacZ* reporter from the same samples presented in
826 A. Data in B were normalized to the level of VqmA-FLAG in A. In B, data represent the
827 average values of biological replicates (*n*=3) and error bars represent SD. Statistical

significance was calculated using a two-tailed Student's t-test. Asterisks as follows: **** denotes p<0.0001.

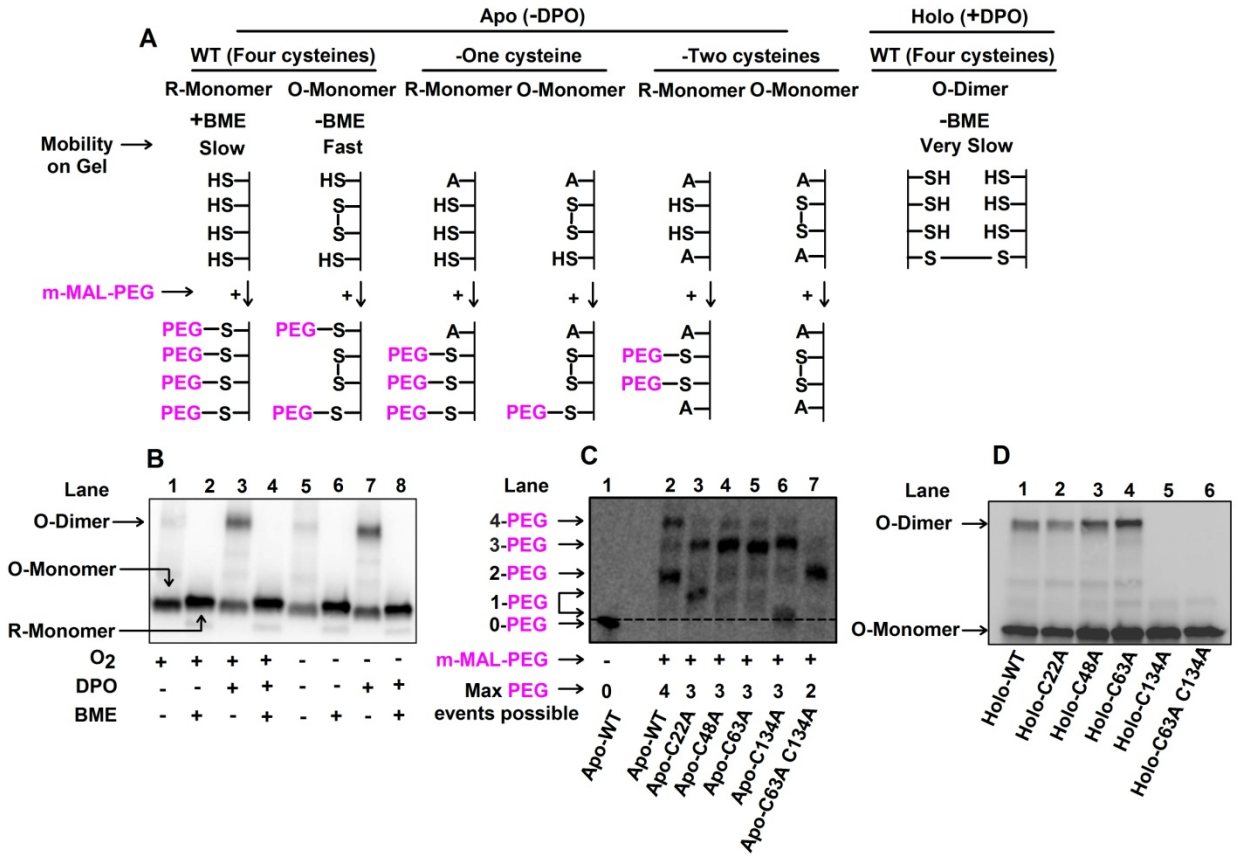

Figure 4. VqmA forms intra- and inter-molecular disulfide bonds in an oxygen- and DPO-dependent manner. **(A)** Schematic depicting the oxidized and reduced forms of VqmA (top) and the strategy employed to interrogate intra-molecular disulfide bond formation by trapping reduced thiols with methoxypolyethylene glycol maleimide (m-MAL-PEG; 5kDa, bottom) (32). **(B)** Western blot showing VqmA-FLAG protein produced by the Δ*vqmA* Δ*tdh V. cholerae* strain carrying p*vqmA-FLAG* following the specified treatments. **(C)** Western blot showing VqmA-FLAG protein produced by the Δ*vqmA* Δ*tdh V. cholerae* strain carrying the designated p*vqmA*-FLAG alleles following treatment with m-MAL-PEG (32) in the absence of DPO. Note that in lanes 3 and 6, the proteins containing 1-PEG modification migrate somewhat differently. We infer the bands to be 1-PEG events by comparison with the 0-PEG event in lane 1 and the 2-PEG event in lane 7. A likely explanation is that the protein containing 1-PEG in lane 6 adopts a more

843 compact conformation than the modified protein in lane 3 and so it migrates faster
844 through the gel (2, 55). The dotted line distinguishes the 0-PEG VqmA from the lowest
845 1-PEG decorated species. **(D)** Western blot showing VqmA-FLAG for the strains in C
846 following supplementation with 25 μM DPO under non-reducing conditions.

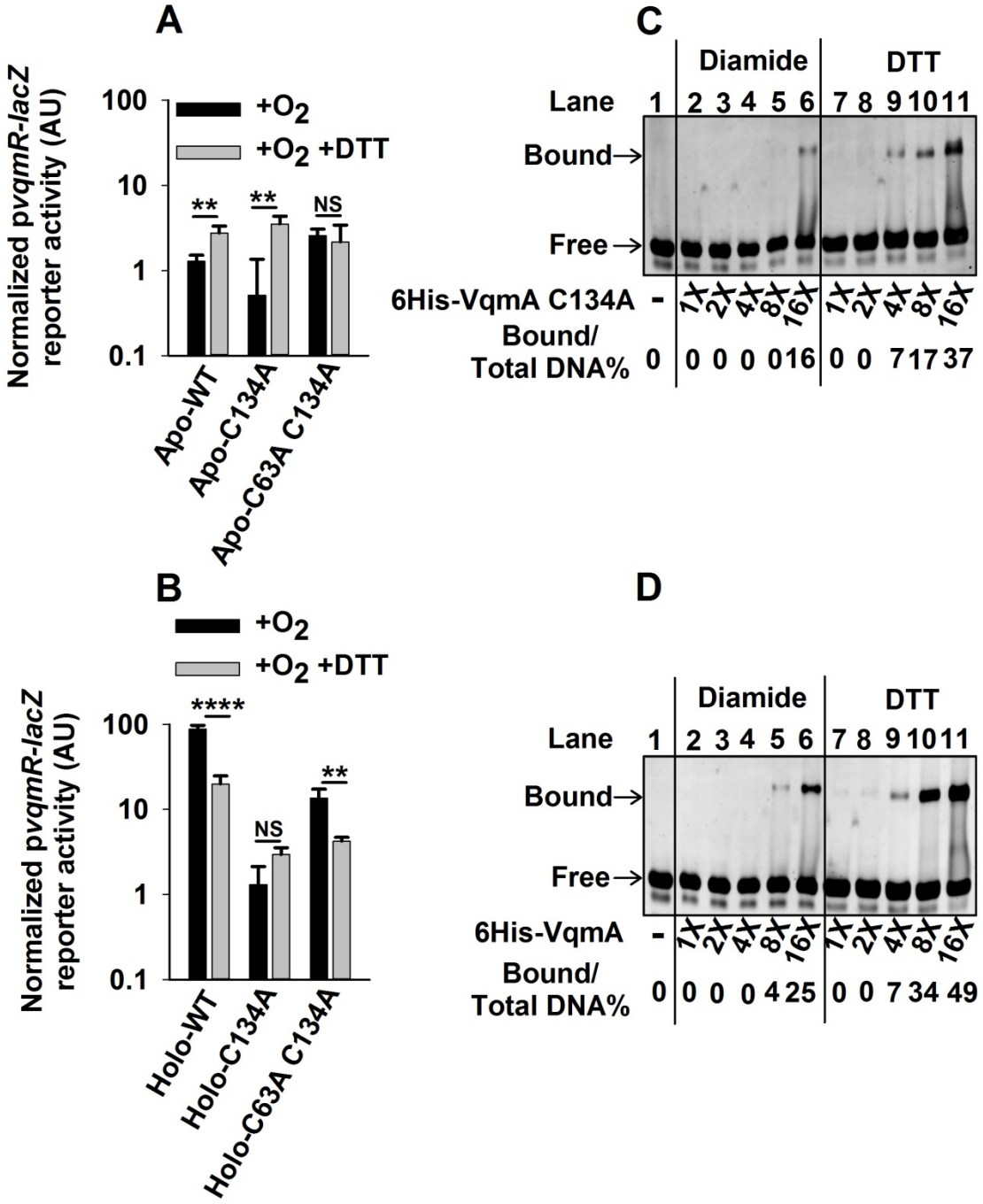

Figure 5. VqmA activity is differentially modulated by the cellular redox environment and intra- and inter-molecular disulfide bonds. **(A)** p*vqmR-lacZ* activity in Δ*vqmA* Δ*tdh V. cholerae* carrying the designated p*vqmA-FLAG* constructs following growth in the presence of O_2 without (black) or with DTT (gray). **(B)** Strains cultured as in A

869 supplemented with 25 μM DPO. **(C)** Electromobility shift analysis (EMSA) of 6His-VqmA
870 C134A binding to *vqmR* promoter DNA. **(D)** EMSA as in C for WT 6His-VqmA. In C and
871 D**,** all lanes contained 35 ng of promoter DNA and, where indicated, dilutions of protein
872 were used with 16X = 2 μg. Bound and free correspond to DNA that is and is not bound
873 to VqmA protein, respectively. As indicated, VqmA had been treated with 10-fold molar
874 excess of diamide or DTT. Data in A and B represent average values of biological
875 replicates (*n*=3) and error bars represent SD. Statistical significance was calculated
876 using a two-tailed Student's t-test. Asterisks as follows: ** denotes $p<0.01$, **** denotes
877 $p<0.0001$, and NS denotes $p>0.05$.

878

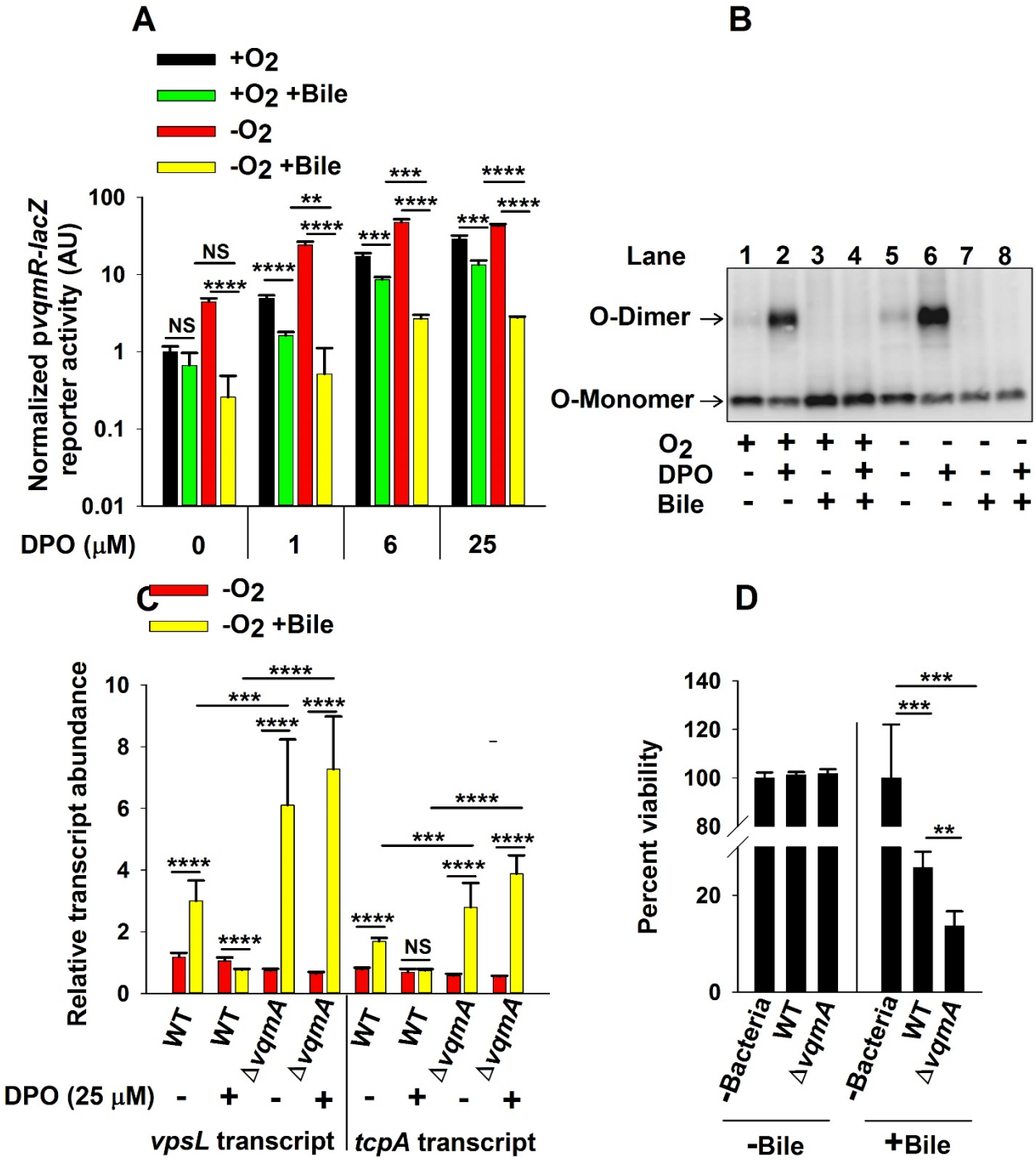

879

880 **Figure 6.** Bile salts disrupt VqmA-DPO-mediated signal transduction and promote *V.*
881 *cholerae* virulence. **(A)** p*vqmR-lacZ* activity in Δ*vqmA* Δ*tdh V. cholerae* carrying p*vqmA-*
882 *FLAG* following 1 h in the presence or absence of O_2, 0.5% (v/v) bile salts, and 0-25 μM
883 DPO or combinations of all three treatments as indicated. **(B)** Western blot showing
884 VqmA-FLAG for the strain in A following the indicated treatments. **(C)** Relative

885 expression levels of *vpsL* and *tcpA* in WT and Δ*vqmA V. cholerae* following the
886 designated treatments. **(D)** Viability of human intestinal CaCo-2 cells in the absence of
887 bacteria or following challenge by WT or Δ*vqmA V. cholerae* and in the presence or
888 absence of 0.05% bile salts. Data in panels A, and D represent average values of
889 biological replicates (*n*=3) and error bars represent SD. Data in panel C represent the
890 average value of three biological replicates and two technical replicates for each sample
891 (*n*=6) and error bars represent SD. Statistical significance was calculated using a two-
892 tailed Student's t-test. Asterisks as follows: ** denotes p<0.01, *** denotes p<0.001, ****
893 denotes p<0.0001, and NS denotes p>0.05.

894

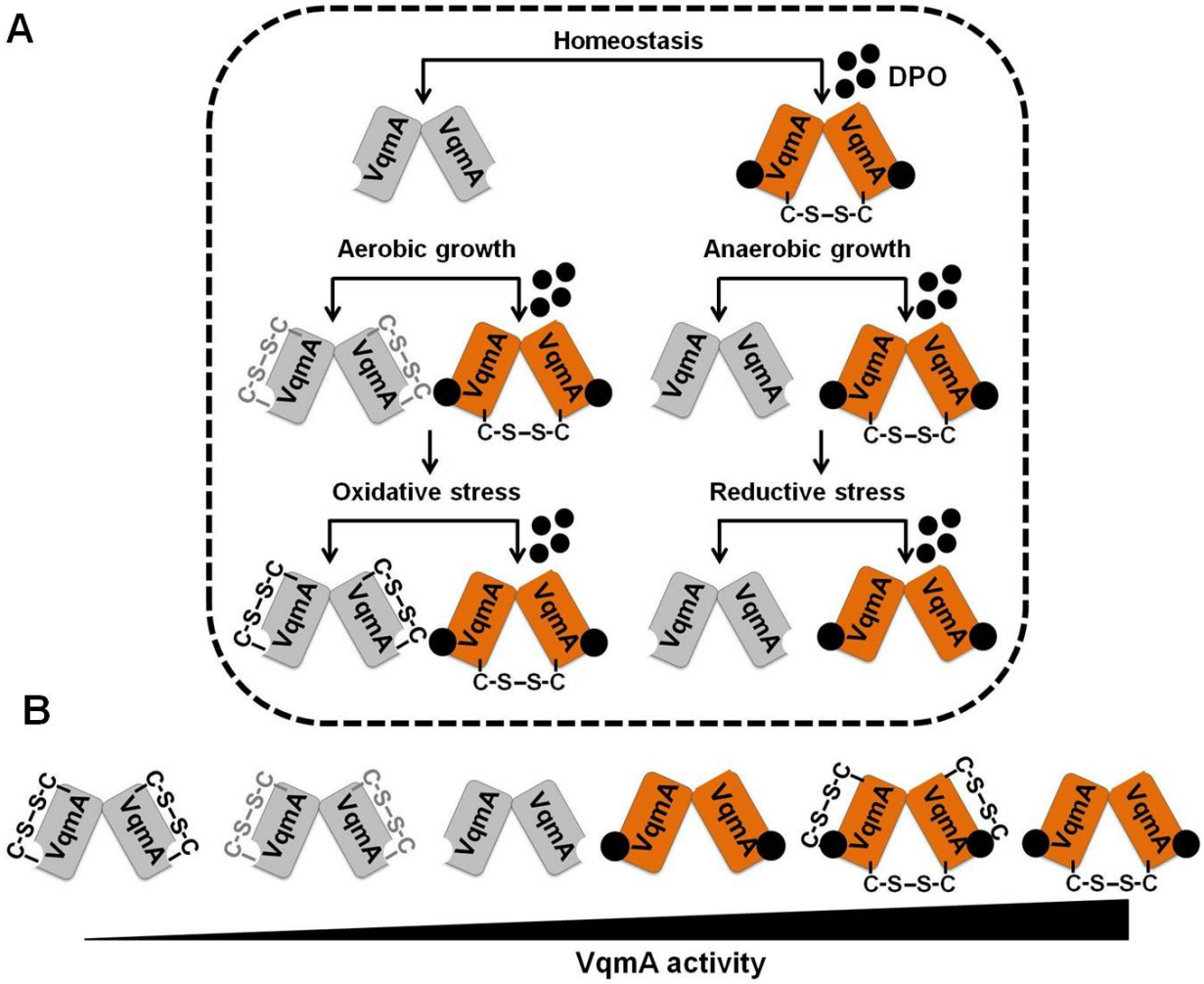

Figure 7. Model depicting VqmA as a hub protein that compiles quorum-sensing, environmental, and host information. **(A)** VqmA can exist in different states *in vivo* depending upon the availability of the DPO ligand and the cellular redox state. Thus, Apo-VqmA forms the C48-C63 intra-molecular disulfide bond that suppresses its ability to bind DNA. Apo-VqmA activity is high under reducing growth conditions in which formation of the intra-molecular C48-C63 bond is inhibited. Holo-VqmA forms the C134-C134 inter-molecular disulfide bond that promotes DNA binding. Reductive stress disrupts the formation of the inter-molecular disulfide bond. We propose that growth in the presence of bile salts imposes reductive stress, disrupts the formation of the C134-C134 inter-molecular disulfide bond, and restricts VqmA DNA binding, thereby promoting virulence and biofilm formation. The gray and black intra-molecular disulfide bonds denote partially-oxidized and fully-oxidized VqmA, respectfully. **(B)** Relative

908 VqmA activity levels as a consequence of disulfide bond formation. For simplicity, the
909 fourth and fifth species in B are not displayed in A.

910

References:

1. **Antelmann, H., and J. D. Helmann.** 2010. Thiol-based redox switches and gene regulation. Antioxid Redox Signal **14:**1049-63.
2. **Bardwell, J. C., K. McGovern, and J. Beckwith.** 1991. Identification of a protein required for disulfide bond formation *in vivo*. Cell **67:**581-9.
3. **Beyer, H. M., P. Gonschorek, S. L. Samodelov, M. Meier, W. Weber, and M. D. Zurbriggen.** 2015. AQUA Cloning: A Versatile and Simple Enzyme-Free Cloning Approach. PLoS One **10:**e0137652.
4. **Braun, M., and L. Thony-Meyer.** 2005. Cytochrome c maturation and the physiological role of c-type cytochromes in *Vibrio cholerae*. J Bacteriol **187:**5996-6004.
5. **Bridges, A. A., and B. L. Bassler.** 2019. The intragenus and interspecies quorum-sensing autoinducers exert distinct control over *Vibrio cholerae* biofilm formation and dispersal. PLoS Biol **17:**e3000429.
6. **Chatterjee, A., P. K. Dutta, and R. Chowdhury.** 2007. Effect of fatty acids and cholesterol present in bile on expression of virulence factors and motility of *Vibrio cholerae*. Infect Immun **75:**1946-53.
7. **Chen, P. R., S. Nishida, C. B. Poor, A. Cheng, T. Bae, L. Kuechenmeister, P. M. Dunman, D. Missiakas, and C. He.** 2009. A new oxidative sensing and regulation pathway mediated by the MgrA homologue SarZ in *Staphylococcus aureus*. Mol Microbiol **71:**198-211.
8. **Chen, X., S. Schauder, N. Potier, A. Van Dorsselaer, I. Pelczer, B. L. Bassler, and F. M. Hughson.** 2002. Structural identification of a bacterial quorum-sensing signal containing boron. Nature **415:**545-9.
9. **Childers, B. M., X. Cao, G. G. Weber, B. Demeler, P. J. Hart, and K. E. Klose.** 2011. N-terminal residues of the *Vibrio cholerae* virulence regulatory protein ToxT involved in dimerization and modulation by fatty acids. J Biol Chem **286:**28644-55.
10. **Cremers, C. M., and U. Jakob.** 2013. Oxidant sensing by reversible disulfide bond formation. J Biol Chem **288:**26489-96.
11. **Cremers, C. M., D. Knoefler, V. Vitvitsky, R. Banerjee, and U. Jakob.** 2014. Bile salts act as effective protein-unfolding agents and instigators of disulfide stress *in vivo*. Proc Natl Acad Sci U S A **111:**E1610-9.
12. **Dalia, A. B.** 2018. Natural Cotransformation and Multiplex Genome Editing by Natural Transformation (MuGENT) of *Vibrio cholerae*. Methods Mol Biol **1839:**53-64.
13. **Dalia, A. B., E. McDonough, and A. Camilli.** 2014. Multiplex genome editing by natural transformation. Proc Natl Acad Sci U S A **111:**8937-42.
14. **Dawson, P. A.** 1998. Bile secretion and the enterohepatic circulation of bile acids. In M. Feldman, M. H. Sleisenger, and B. F. Scharschmidt (ed.), Sleisenger and Fordtran's gastrointestinal and liver disease: pathophysiology/diagnosis/management, 6th ed. W. B. Saunders, Co., Philadelphia, PA.**:**1052-1063.

954 15. **Escobar, L. E., S. J. Ryan, A. M. Stewart-Ibarra, J. L. Finkelstein, C. A. King,**
955 **H. Qiao, and M. E. Polhemus.** 2015. A global map of suitability for coastal *Vibrio*
956 *cholerae* under current and future climate conditions. Acta Trop **149:**202-11.
957 16. **Falke, J. J., and D. E. Koshland, Jr.** 1987. Global flexibility in a sensory
958 receptor: a site-directed cross-linking approach. Science **237:**1596-600.
959 17. **Fong, J. C. N., K. A. Syed, K. E. Klose, and F. H. Yildiz.** 2010. Role of Vibrio
960 polysaccharide (*vps*) genes in VPS production, biofilm formation and *Vibrio*
961 *cholerae* pathogenesis. Microbiology **156:**2757-2769.
962 18. **Fuchs, S., J. Pane-Farre, C. Kohler, M. Hecker, and S. Engelmann.** 2007.
963 Anaerobic gene expression in *Staphylococcus aureus*. J Bacteriol **189:**4275-89.
964 19. **Garcia-Quintanilla, M., A. I. Prieto, L. Barnes, F. Ramos-Morales, and J.**
965 **Casadesus.** 2006. Bile-induced curing of the virulence plasmid in *Salmonella*
966 *enterica* serovar Typhimurium. J Bacteriol **188:**7963-5.
967 20. **Hammer, B. K., and B. L. Bassler.** 2003. Quorum sensing controls biofilm
968 formation in *Vibrio cholerae*. Mol Microbiol **50:**101-4.
969 21. **Higgins, D. A., M. E. Pomianek, C. M. Kraml, R. K. Taylor, M. F.**
970 **Semmelhack, and B. L. Bassler.** 2007. The major *Vibrio cholerae* autoinducer
971 and its role in virulence factor production. Nature **450:**883-6.
972 22. **Huang, X., O. P. Duddy, J. E. Silpe, J. E. Paczkowski, J. Cong, B. R. Henke,**
973 **and B. L. Bassler.** 2020. Mechanism underlying autoinducer recognition in the
974 *Vibrio cholerae* DPO-VqmA quorum-sensing pathway. J Biol Chem **295:**2916-
975 2931.
976 23. **Hung, D. T., and J. J. Mekalanos.** 2005. Bile acids induce cholera toxin
977 expression in *Vibrio cholerae* in a ToxT-independent manner. Proc Natl Acad Sci
978 U S A **102:**3028-33.
979 24. **Hung, D. T., J. Zhu, D. Sturtevant, and J. J. Mekalanos.** 2006. Bile acids
980 stimulate biofilm formation in *Vibrio cholerae*. Mol Microbiol **59:**193-201.
981 25. **Joelsson, A., B. Kan, and J. Zhu.** 2007. Quorum sensing enhances the stress
982 response in *Vibrio cholerae*. Appl Environ Microbiol **73:**3742-6.
983 26. **Johansson, M. E., H. Sjovall, and G. C. Hansson.** 2013. The gastrointestinal
984 mucus system in health and disease. Nat Rev Gastroenterol Hepatol **10:**352-61.
985 27. **Jung, S. A., C. A. Chapman, and W. L. Ng.** 2015. Quadruple quorum-sensing
986 inputs control *Vibrio cholerae* virulence and maintain system robustness. PLoS
987 Pathog **11:**e1004837.
988 28. **Kelly, R. C., M. E. Bolitho, D. A. Higgins, W. Lu, W. L. Ng, P. D. Jeffrey, J. D.**
989 **Rabinowitz, M. F. Semmelhack, F. M. Hughson, and B. L. Bassler.** 2009. The
990 *Vibrio cholerae* quorum-sensing autoinducer CAI-1: analysis of the biosynthetic
991 enzyme CqsA. Nat Chem Biol **5:**891-5.
992 29. **Koestler, B. J., and C. M. Waters.** 2014. Bile acids and bicarbonate inversely
993 regulate intracellular cyclic di-GMP in *Vibrio cholerae*. Infect Immun **82:**3002-14.
994 30. **Kosower, N. S., and E. M. Kosower.** 1995. Diamide: an oxidant probe for thiols.
995 Methods Enzymol **251:**123-33.
996 31. **Krishnan, H. H., A. Ghosh, K. Paul, and R. Chowdhury.** 2004. Effect of
997 anaerobiosis on expression of virulence factors in *Vibrio cholerae*. Infect Immun
998 **72:**3961-7.

32. **Landeta, C., L. McPartland, N. Q. Tran, B. M. Meehan, Y. Zhang, Z. Tanweer, S. Wakabayashi, J. Rock, T. Kim, D. Balasubramanian, R. Audette, M. Toosky, J. Pinkham, E. J. Rubin, S. Lory, G. Pier, D. Boyd, and J. Beckwith.** 2019. Inhibition of *Pseudomonas aeruginosa* and *Mycobacterium tuberculosis* disulfide bond forming enzymes. Mol Microbiol **111:**918-937.
33. **Lee, K. M., Y. Park, W. Bari, M. Y. Yoon, J. Go, S. C. Kim, H. I. Lee, and S. S. Yoon.** 2012. Activation of cholera toxin production by anaerobic respiration of trimethylamine N-oxide in *Vibrio cholerae*. J Biol Chem **287:**39742-52.
34. **Liu, Z., A. Hsiao, A. Joelsson, and J. Zhu.** 2006. The transcriptional regulator VqmA increases expression of the quorum-sensing activator HapR in *Vibrio cholerae*. J Bacteriol **188:**2446-53.
35. **Liu, Z., M. Yang, G. L. Peterfreund, A. M. Tsou, N. Selamoglu, F. Daldal, Z. Zhong, B. Kan, and J. Zhu.** 2010. *Vibrio cholerae* anaerobic induction of virulence gene expression is controlled by thiol-based switches of virulence regulator AphB. Proc Natl Acad Sci U S A **108:**810-5.
36. **Lowden, M. J., K. Skorupski, M. Pellegrini, M. G. Chiorazzo, R. K. Taylor, and F. J. Kull.** 2010. Structure of *Vibrio cholerae* ToxT reveals a mechanism for fatty acid regulation of virulence genes. Proc Natl Acad Sci U S A **107:**2860-5.
37. **Mashruwala, A. A., S. Bhatt, S. Poudel, E. S. Boyd, and J. M. Boyd.** 2016. The DUF59 Containing Protein SufT Is Involved in the Maturation of Iron-Sulfur (FeS) Proteins during Conditions of High FeS Cofactor Demand in *Staphylococcus aureus*. PLoS Genet **12:**e1006233.
38. **Masuda, S., C. Dong, D. Swem, A. T. Setterdahl, D. B. Knaff, and C. E. Bauer.** 2002. Repression of photosynthesis gene expression by formation of a disulfide bond in CrtJ. Proc Natl Acad Sci U S A **99:**7078-83.
39. **Miller, M. B., K. Skorupski, D. H. Lenz, R. K. Taylor, and B. L. Bassler.** 2002. Parallel quorum sensing systems converge to regulate virulence in *Vibrio cholerae*. Cell **110:**303-14.
40. **Muras, V., P. Dogaru-Kinn, Y. Minato, C. C. Hase, and J. Steuber.** 2016. The Na+-Translocating NADH:Quinone Oxidoreductase Enhances Oxidative Stress in the Cytoplasm of *Vibrio cholerae*. J Bacteriol **198:**2307-17.
41. **Nozaki, S., and H. Niki.** 2019. Exonuclease III (XthA) Enforces *In Vivo* DNA Cloning of *Escherichia coli* To Create Cohesive Ends. J Bacteriol **201**.
42. **Oktiabrskii, O. N., Smirnova, G. V.** 2012. Redox potential changes in bacterial cultures under stress conditions. Microbiology **81:**131-142.
43. **Olive, A. J., R. Kenjale, M. Espina, D. S. Moore, W. L. Picking, and W. D. Picking.** 2007. Bile salts stimulate recruitment of IpaB to the *Shigella flexneri* surface, where it colocalizes with IpaD at the tip of the type III secretion needle. Infect Immun **75:**2626-9.
44. **Ottemann, K. M., and J. J. Mekalanos.** 1996. The ToxR protein of *Vibrio cholerae* forms homodimers and heterodimers. J Bacteriol **178:**156-62.
45. **Papenfort, K., and B. L. Bassler.** 2016. Quorum sensing signal-response systems in Gram-negative bacteria. Nat Rev Microbiol **14:**576-88.
46. **Papenfort, K., K. U. Forstner, J. P. Cong, C. M. Sharma, and B. L. Bassler.** 2015. Differential RNA-seq of *Vibrio cholerae* identifies the VqmR small RNA as a regulator of biofilm formation. Proc Natl Acad Sci U S A **112:**E766-75.

1045 47. **Papenfort, K., J. E. Silpe, K. R. Schramma, J. P. Cong, M. R.**
1046 **Seyedsayamdost, and B. L. Bassler.** 2017. A *Vibrio cholerae* autoinducer-
1047 receptor pair that controls biofilm formation. Nat Chem Biol **13:**551-557.
1048 48. **Parashar, V., C. Aggarwal, M. J. Federle, and M. B. Neiditch.** 2015. Rgg
1049 protein structure-function and inhibition by cyclic peptide compounds. Proc Natl
1050 Acad Sci U S A **112:**5177-82.
1051 49. **Pereira, C. S., J. A. Thompson, and K. B. Xavier.** 2013. AI-2-mediated
1052 signalling in bacteria. FEMS Microbiol Rev **37:**156-81.
1053 50. **Plecha, S. C., and J. H. Withey.** 2015. Mechanism for inhibition of *Vibrio*
1054 *cholerae* ToxT activity by the unsaturated fatty acid components of bile. J
1055 Bacteriol **197:**1716-25.
1056 51. **Repetto, G., A. del Peso, and J. L. Zurita.** 2008. Neutral red uptake assay for
1057 the estimation of cell viability/cytotoxicity. Nat Protoc **3:**1125-31.
1058 52. **Rossius, M., F. Hochgrafe, and H. Antelmann.** 2018. Thiol-Redox Proteomics
1059 to Study Reversible Protein Thiol Oxidations in Bacteria. Methods Mol Biol
1060 **1841:**261-275.
1061 53. **Schauder, S., and B. L. Bassler.** 2001. The languages of bacteria. Genes Dev
1062 **15:**1468-80.
1063 54. **Schauder, S., K. Shokat, M. G. Surette, and B. L. Bassler.** 2001. The LuxS
1064 family of bacterial autoinducers: biosynthesis of a novel quorum-sensing signal
1065 molecule. Mol Microbiol **41:**463-76.
1066 55. **Scheele, G., and R. Jacoby.** 1982. Conformational changes associated with
1067 proteolytic processing of presecretory proteins allow glutathione-catalyzed
1068 formation of native disulfide bonds. J Biol Chem **257:**12277-82.
1069 56. **Suckow, G., P. Seitz, and M. Blokesch.** 2011. Quorum sensing contributes to
1070 natural transformation of *Vibrio cholerae* in a species-specific manner. J Bacteriol
1071 **193:**4914-24.
1072 57. **Taylor, R. K., V. L. Miller, D. B. Furlong, and J. J. Mekalanos.** 1987. Use of
1073 *phoA* gene fusions to identify a pilus colonization factor coordinately regulated
1074 with cholera toxin. Proc Natl Acad Sci U S A **84:**2833-7.
1075 58. **Trotter, E. W., and C. M. Grant.** 2002. Thioredoxins are required for protection
1076 against a reductive stress in the yeast *Saccharomyces cerevisiae*. Mol Microbiol
1077 **46:**869-78.
1078 59. **Waters, C. M., and B. L. Bassler.** 2005. Quorum sensing: cell-to-cell
1079 communication in bacteria. Annu Rev Cell Dev Biol **21:**319-46.
1080 60. **Weber, G. G., and K. E. Klose.** 2011. The complexity of ToxT-dependent
1081 transcription in *Vibrio cholerae*. Indian J Med Res **133:**201-6.
1082 61. **Winzer, K., K. R. Hardie, N. Burgess, N. Doherty, D. Kirke, M. T. G. Holden,**
1083 **R. Linforth, K. A. Cornell, A. J. Taylor, P. J. Hill, and P. Williams.** 2002. LuxS:
1084 its role in central metabolism and the *in vitro* synthesis of 4-hydroxy-5-methyl-
1085 3(2H)-furanone. Microbiology **148:**909-922.
1086 62. **Wu, H., M. Li, H. Guo, H. Zhou, B. Li, Q. Xu, C. Xu, F. Yu, and J. He.** 2019.
1087 Crystal structure of the *Vibrio cholerae* VqmA-ligand-DNA complex provides
1088 insight into ligand-binding mechanisms relevant for drug design. J Biol Chem
1089 **294:**2580-2592.

1090 63. **Wu, H., M. Li, C. Peng, Y. Yin, H. Guo, W. Wang, Q. Xu, H. Zhou, C. Xu, F. Yu,**
1091 **and J. He.** 2019. Large conformation shifts of *Vibrio cholerae* VqmA dimer in the
1092 absence of target DNA provide insight into DNA-binding mechanisms of LuxR-
1093 type receptors. Biochem Biophys Res Commun **520:**399-405.
1094 64. **Xue, Y., F. Tu, M. Shi, C. Q. Wu, G. Ren, X. Wang, W. Fang, H. Song, and M.**
1095 **Yang.** 2016. Redox pathway sensing bile salts activates virulence gene
1096 expression in *Vibrio cholerae*. Mol Microbiol **102:**909-924.
1097 65. **Yang, M., Z. Liu, C. Hughes, A. M. Stern, H. Wang, Z. Zhong, B. Kan, W.**
1098 **Fenical, and J. Zhu.** 2013. Bile salt-induced intermolecular disulfide bond
1099 formation activates *Vibrio cholerae* virulence. Proc Natl Acad Sci U S A
1100 **110:**2348-53.
1101 66. **Zheng, L., C. J. Kelly, and S. P. Colgan.** 2015. Physiologic hypoxia and oxygen
1102 homeostasis in the healthy intestine. A Review in the Theme: Cellular Responses
1103 to Hypoxia. Am J Physiol Cell Physiol **309:**C350-60.
1104 67. **Zheng, M., F. Aslund, and G. Storz.** 1998. Activation of the OxyR transcription
1105 factor by reversible disulfide bond formation. Science **279:**1718-21.
1106 68. **Zhu, J., and J. J. Mekalanos.** 2003. Quorum sensing-dependent biofilms
1107 enhance colonization in *Vibrio cholerae*. Dev Cell **5:**647-56.
1108 69. **Zhu, J., M. B. Miller, R. E. Vance, M. Dziejman, B. L. Bassler, and J. J.**
1109 **Mekalanos.** 2002. Quorum-sensing regulators control virulence gene expression
1110 in *Vibrio cholerae*. Proc Natl Acad Sci U S A **99:**3129-34.
1111
1112